1-1-2015

# Novel Pulsatile Cardiac Assist Pump

Lakshmi Mohanadas
*Wayne State University,*

**NOVEL PULSATILE CARDIAC ASSIST PUMP**

by

**LAKSHMI MOHANADAS**

**THESIS**

Submitted to the Graduate School

of Wayne State University,

Detroit, Michigan

in partial fulfillment of the requirements

for the degree of

**MASTER OF SCIENCE**

2015

MAJOR: BIOMEDICAL ENGINEERING

Approved By:

_____

Advisor Date

**DEDICATION**

***To***

***My Parents and friends***

## ACKNOWLEDGEMENTS

I owe a great thanks to a great many people who has helped, supported and encouraged me throughout this journey. My sincere gratitude to my advisor Dr. Auner for extending his constant interest, support, genuine apprehension and encouragement for the success of this project. I would also like to thank Dr. Huang for rendering his technical support and helping me in the construction of this study. His patience and scholarly knowledge made the work more enjoyable. Thanks are due to my Department of Biomedical Engineering, Wayne State University for putting forward guidelines for the timely completion of the thesis.

I also thank my committee members: Dr. M. Kavadia and Dr. M. Brusatori for their valuable time and readily accepting to participate in my thesis.

I thank the Almighty, who is the source of this life and provided me with the strength, knowledge and wisdom.

I render my regards to my beloved parents and friends for their untiring love and inspiration which helped me carry out my task.

## TABLE OF CONTENTS

## LIST OF TABLES

## LIST OF FIGURES

# CHAPTER 1

# INTRODUCTION

Cardiac pumps are revolutionary devices which assist the failing heart function. Over the decade many cardiovascular pumps have been developed to assist the heart. These devices are generally mechanical pumps which help in efficient blood circulation. Due to the increase of cardiac complications after a surgery and the number of patients suffering from heart functioning problems, the demand of heart assistive pumps has also increased in the market which can efficiently increase the heart functioning rate and there by enhance the patient's condition. There are two types of patients who generally need the use of a pump to support the function of their heart. One, those who need immediate assistance after an heart attack or a heart surgery and two, those who are waiting for a heart transplant and they have long wait time. This wait time till transplantation is called as bridge to transplantation. Sometimes these pumps are also used as end therapy, that is the pump is used to provide good quality of life till the recovery of the patient and no transplantation occurs. This usage is also known as bridge to recovery.

In general, the blood pumps are classified on the basis of their mechanical action. The two such categories are: displacement pump and rotary pump [1]. Displacement pumps work on the basis of energy transfer due to periodic changes whereas a rotary pump changes the velocity of the impeller vanes. Rotary pumps become more advantageous over displacement pumps when large volume flow at low pressure is required. But when the low volumetric flow is required with high pressure, displacement pumps are preferred. Displacement pumps are vastly used in the medical field over the past decades for

cardiopulmonary bypass in heart lung machines and in the dialysis machines. These pumps have been widely in use due to their simplicity and low cost. But the major disadvantage caused by them is blood damage and particulate spallation.

On the contrary rotary pumps are more advantageous over the displacement pumps as they possess less blood damage, smaller in size, better transportability, and absence of spallation. Due to all these advantages over displacement pumps, centrifugal pumps, a type of rotary pump, is gaining lot of market in the cardiopulmonary bypass application. But due to the use of rollers, these can be used upto a time limit of 4 hours as there is risk of blood cell damage and to compensate high doses of anticoagulation drugs are also used. These are used to assist patients after an open heart surgery who suffers from low cardiac output known as low output syndrome (LOS) but fails to do so. Hence in treatment more of inotropic and vasoactive drugs are used.

A number of different types of rotary and displacement pumps are still used as ventricular support system. Micro-axial pump is one such type from rotary pumps group which are introduce through femoral artery and its inflow cannula is place through the aortic valve to the left ventricle. The first axial-type blood pump was introduced into the market by Johnson & Johnson (Division of Ethicon Inc., Arlington, TX, USA) under the name of 'Hemopump'[1].

Another type is the pneumatic displacement pump which is introduced through thoracotomy. These pumps possess the risk of skin infection at their penetration sites. Also the patient has less mobility due to the bulkiness and the moving consoles. To compensate old mechanical support systems, fully implantable electro-mechanical left ventricular assist devices (LVADs) have been developed. Two such systems that are

currently available are the NOVACOR (Baxter Healthcare Corp., Deerfield, IL, USA)[3][4] and the HeartMate (Thermo Cardiosystems Inc., Woburn, MA, USA)[5].

Rotary pumps are classified generally into three categories according to the impeller geometry: Radial (centrifugal), axial and diagonal. Axial flow pumps are efficient at low pressure differences and generate high volumetric flow whereas a radial pump is designed to produce low flow rates at high pressure. Diagonal pumps also known as mixed flow systems, generally operate at high pressure to provide high flow rate.

As stated rotary pumps have a number of theoretical and practical advantages over the displacement types. They have low blood trauma, lesser anti coagulation levels and therefore lesser chances of hemorrhage. Also depending on the design, they can also be coated with heparin. A detailed tree chart description of different types of pumps available in the market is provided in figure 1 and figure 2 [1]. A further more detailed description of the devices in the market is given in tables 1,2,3 and 4. These tables shows the description of the pumps mentioned in the figure 1 and 2. The pump name and the company which prototyped it along with the application, the position of the pump, what type of support does the pump offer and for what duration the pump is used is provided in the table. Table 2 specifically enumerates the different types of centrifugal pumps in the market with their developers and the duration for which they are used.

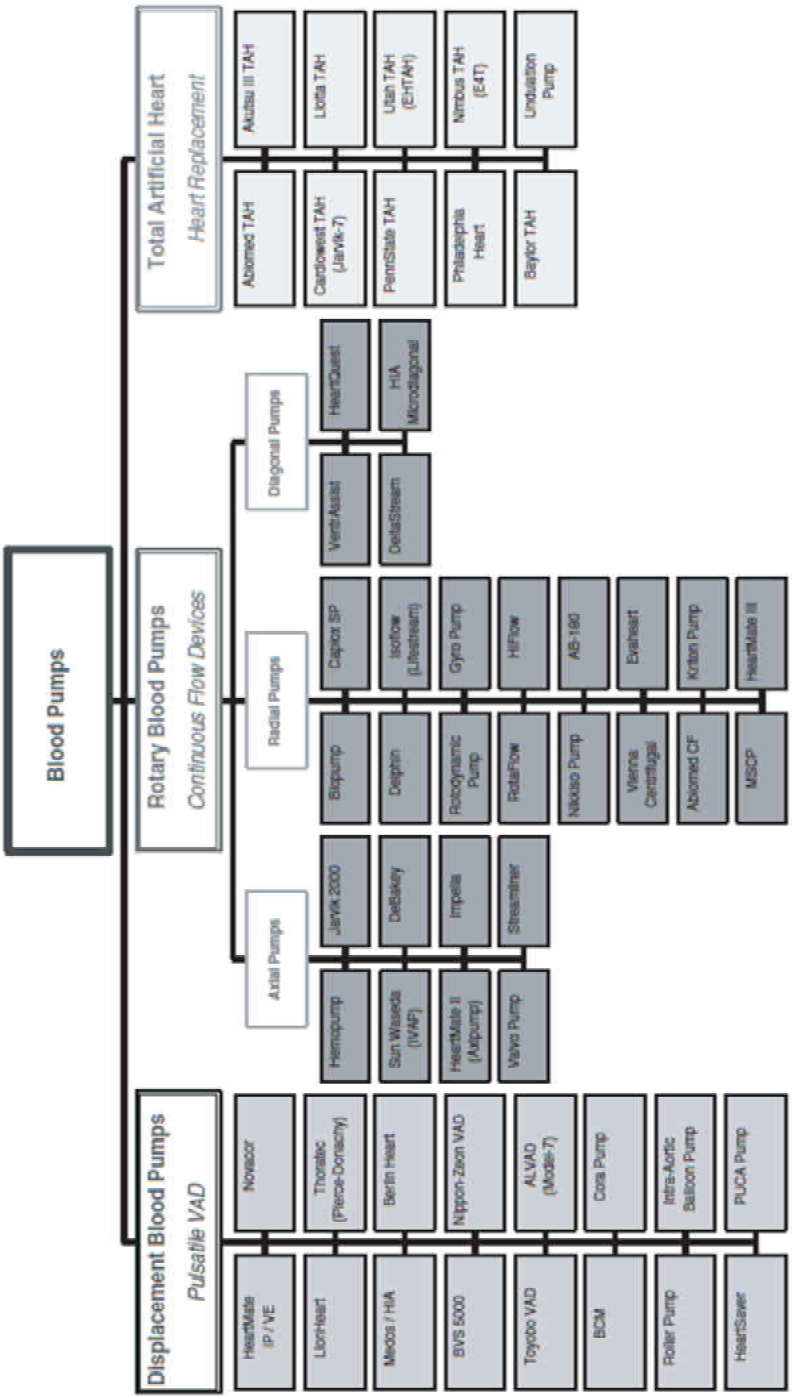


Fig 1: Type of Blood pumps [1]

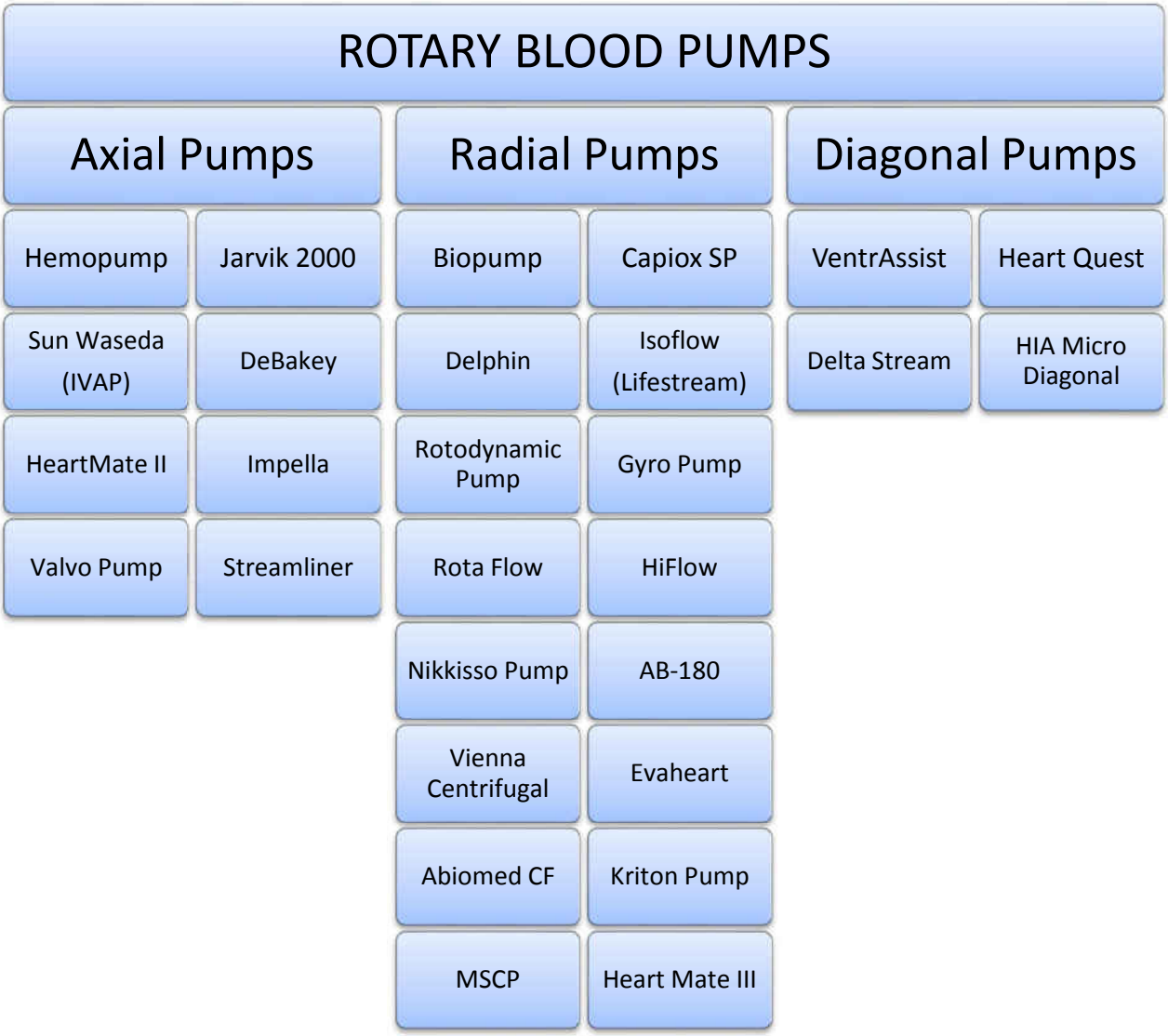


Fig 2: Types of Rotary Pumps in the market

Table 1: Axial Blood Pumps [1]

| Pump | Organization | Application | Position | Support | Duration |
|---|---|---|---|---|---|
| Hemopump | Medtronic Inc., Minneapolis, MN, USA | Postcardiotomy/ coronary surgery | Implantable intra-arterial/ transvalvular (aortic valve) | Left ventricular | Short term/ medium term |
| Jarvik 2000 | Jarvik Heart Inc., Oxford Heart Centre, USA/UK | VAD/BTT | Implantable intraventricular | Left ventricular | Long term |
| IVAP | Sun Medical Co., Waseda University, Tokyo, Japan | VAD/BTT | Implantable intraventricular | Left ventricular | Long term |
| DeBakey VAD | MicroMed Technology Inc., Texas, USA | VAD/BTT | Fully implantable abdominal | Left ventricular | Long term |
| HeartMate II | TCI/Nimbus Inc./ Pittsburgh University, Pennsylvania USA | VAD/BTT | Implantable abdominal | Left/right ventricular | Long term |
| Impella | Impella, Cardiotechnik AG Aachen, Germany | Minimal invasive heart surgery | Fully implantable intraventricular | Left/right ventricular | Short term (< 6 h) |
| Valvo Pump | Keio University, Hokkaido University, Tokyo, Japan | VAD/similar to valve replacement | Implantable transvalvular | Left/right ventricular | Medium term |
| Streamliner | McGowan Center, Pittsburgh University, Pennsylvania USA | VAD/BTT | Implantable abdominal | Left/right ventricular | Long term |

VAD: Ventricular Assist Device; BTT: Bridge to transplant

Table 2: Centrifugal pumps [1]

| Pump | Organization | Application | Position | Support | Duration |
|---|---|---|---|---|---|
| Bio-Pump | Medtronic Biomedicus Inc., Minneapolis, | Postcardiotomy/ CPB | Extracorporeal | Left/right ventricular | Short term |
| Capiox | Terumo Corporation Tokyo, Japan | CPB/postcardiotomy | Extracorporeal | Left/right ventricular | Short term |
| Sarns Delphin | Sarns/3M Health Care, Ann Arbor, MI, USA | Postcardiotomy | Extracorporeal | Left/right ventricular | Short term |
| Isoflow (Lifestream) | Bard Cardiopulmonary Products/St Jude Medical Inc., Haverhill, | CPB | Extracorporeal | Left/right ventricular | Short term |
| RotaFlow | JOSTRA Medizintechnik AG Hirrlingen, Germany | CPB/postcardiotomy | Extracorporeal | Left/right ventricular | Short term |
| Nikkiso | Nikkiso Co. Ltd Tokyo, Japan | CPB | Paracorporeal | Left/right ventricular | Short term |
| HiFlow | HIA/Medos, GmbH Aachen, Germany | CPB/postcardiotomy | Extracorporeal | Left/right ventricular | Short term |
| Rotodynamic | Cleveland Clinic Foundation, OH, USA | VAD | Implantable | Left/right ventricular | Long term |
| Gyro | Baylor College of Medicine, Houston, TX, USA | VAD /CPB | Implantable/ paracorporeal | Left/right ventricular | Long term to Medium term |
| AB-180 | Cardiac Assist Technologies Inc. Pittsburgh, PA, USA | VAD postcardiotomy | Implantable/ Thoracic cavity | Left ventricular | Short term Medium term |
| Vienna | Vienna University Vienna, Austria | VAD | Implantable/ thoracic cavity | Left/right ventricular | Long term |

| | | | | | |
|---|---|---|---|---|---|
| Evaheart | Sun Medical Corp Pittsburgh University Japan/USA | VAD<br>BTT | Implantable/ thoracic cavity | Left ventricular | Long term |
| Abiomed CF | Abiomed Inc., Danvers, MA, USA | VAD | Implantable | Left/right ventricular | Long term |
| Kriton | Kriton Medical Inc., Citrus Heights, CA, USA. | VAD | Implantable/ left ventricular apex | Left ventricular | Long term |
| MSCP | Terumo Corporation Setsunan University Japan | VAD | Implantable/ thoracic cavity | Left ventricular | Long term |

Table: 3 Diagonal pumps[1]

| **Pump** | **Organization** | **Application** | **Position** | **Support** | **Duration** |
|---|---|---|---|---|---|
| VentrAssist | Micromedical Ltd, Sydney University, Australia | VAD/ BTT | Implantable/ abdominal | Left/right ventricular | Long term |
| HeartQuest | MedQuest Products Inc., Salt Lake City, UT, USA. | VAD/ TAH | Implantable/ Abdominal | Left/right ventricular | Long term (> 10 years) |
| DeltaStream | HIA/Medos, GmbH Aachen, Germany | CPB/VAD/<br>ECMO, etc. | Extracorporeal | Left/right ventricular | Short term |

Table 4 : Detailed description of different types of axial pumps [1]

| PUMP | WEIGHT/ SIZE | FLOW RATE (L/MIN) | ROTATIONAL SPEED (RPM) | POWER REQ (WATTS) | TYPES OF BEARINGS | TYPES OF SEALS | TYPES OF SENSORS | ADDITIONAL FEATURES | STAGE OF DEVELOPMENT |
|---|---|---|---|---|---|---|---|---|---|
| Hemopump  | 6g/5cc | 4.5 | 25000 | 70 | Purge fluid - lubricated hydrostatic journal bearings | Purged seal system Dextrose solution as purge fluid | External controller in console | Impeller (Archimedes screw) is driven by a flexible cable, which is rotated by a paracorporeal motor<br><br>Pump introduced through femoral artery<br><br>Application in minimal invasive heart surgery<br><br>Not produced anymore | Clinical use (since 1990) |
| Jarvik 2000  | 90g/25cc | 6 | 10000-160000 | 7-10 | Blood-immersed ceramic bearings | No seals | External microprocessor-based automatic motor controller regulating pump speed according to physical demands Control modes: Heart rate responsive mode or fixed rate mode possible | Rotor magnets inside impeller<br><br>Electrical wires penetrate scalp<br><br>Pediatric type available | Animal experiments |
| IVAP | 170 g | 5 | 9 | 8 | Pressure-grooved ceramic journal bearings Bearings | First: purged - lip seal (silicone) | External blood pump controller | Pump introduced through LV apex, outflow across | Animal expt |

| | | | | | | | | | |
|---|---|---|---|---|---|---|---|---|---|
| 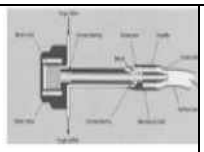 | | | | | cooled by purge fluid Bearings acting as a miniature viscous pump for the purge fluid (spiral/ helix grooves on bearings surface) | Later: Cool seal system | | aortic valve | |
| DeBakye VAD  | 95g/ 15cc | 5 | 7500-120000 | 6 | Ceramic bearings (blood lubricated) located as the conjunction of the impeller with the flow straightener (front) and flow diffuser (rare) | No seals | Micro-controller coupled with internal battery powered by TETS | Rotor magnets are located (hermetically sealed) inside the impeller vanes CFD - based design Prices < USD 10000 | Clinical trial |
| HeartMate II 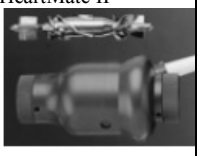 | 160g/62cc | 6 | 6000-13000 | 10 | Ceramic bearings, similar to ball cup jewel bearings, acting against radial and axial thrust Blood immersed Ceramics and diamond coatings preferred bearing materials | No seals | Electronic ( external) controller modulates pump speed according to physiological demands | Rotor magnets are located in the hub of the pumps rotor<br><br>TETS will be used in the future | Ready for clinical trial |
| Impella  | 5g/2cc | 4.5 | 30000 | 12 | Ball bearings located inside motor chamber | Polymeric lip seal | Internal pressure sensors for monitoring, external controller integrade in console | Pump introduced through the femoral artery<br><br>Integrated electric motor<br><br>Long-term pump in developme | Clinical use |

| | | | | | | | | | |
|---|---|---|---|---|---|---|---|---|---|
| | | | | | | | | nt<br>Price < US $1000 | |
| Valvo Pump<br> 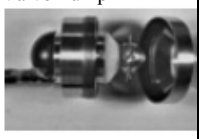 | 138g/40cc | 5 | 9000 | 26 | Miniature ball bearings | Ferrofluidic shaft seal<br><br>Seal ring: Nd-Fe-B magnet<br><br>Ferrofluid: ferricolloid HC-50 | Motor speed is determined by counting pulses from the Hall sensors in the motor | Myocardium is used as pump housing<br><br>Pump may also be used in grafts<br><br>Motor shaft is glued to the rotor | Laboratory |
| Streamliner<br> 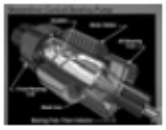 | | | | | Magnetically levitated bearings<br><br>Conical in shape<br><br>Blood lubricated and biocompatible bearings | No seals | Internal and external controller coupled with TETS<br><br>Hybrid controller architecture | Computationally optimized impeller geometry<br><br>CFD-based design | Laboratory |

Table 5: Detailed description of different types of centrifugal pumps [1]

| **PUMP** | **WEIGHT/SIZE** | **FLOW RATE (L/MIN)** | **ROTATIONAL SPEED (RPM)** | **POWER REQ (WATTS)** | **TYPES OF BEARINGS** | **TYPES OF SEALS** | **TYPES OF SENSORS** | **ADDITIONAL FEATURES** | **STAGE OF DEVELOPMENT** |
|---|---|---|---|---|---|---|---|---|---|
| Bio- Pump<br>  | 200g/87cc | 6 | 5 | 8 | Polycarbonate journal bearing | Flexible polymeric seal | Bio-console: electromagnetic flow measurement and pump speed controller | Rotating cone type pump<br><br>Constraint force Vortex pump<br><br>Bioactive surface available for improved biocompatibility<br><br>BP- AT: Adult biopump BP50 pediatric biopump Frequently | Clinical use (greater than 20 years) |

| | | | | | | | | | |
|---|---|---|---|---|---|---|---|---|---|
| | | | | | | | | used as reference pump for comparison studies | |
| Capiox  | 46cc | 5 | 3000 | | Ball bearings | Polymeric lip seal | Auto flow cruise control system adjusts rotational speed to desired flow rate<br><br>Ultrasonic Doppler flow meter. | Straight-path Rotor reduces pump speed without the decreasing hydraulic efficiency resulting in less hemolysis<br><br>Rotor powered by magnetic coupling<br><br>Automatic priming function allows pulsatile flow mode | Clinical use |
| Sarns Delphin 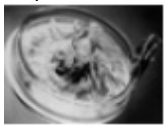 | 130g | 9 | 3600 | | Ball bearings | Polymeric lip seal<br><br>Problems with seal disruption encountered in clinical use | Microcomputer-based control console<br><br>Doppler flow sensor | Pulsatile flow mode option<br><br>Open impeller with straight vanes<br><br>Activated by magnetic coupling | Clinical use (greater than 10 years) |
| Isoflow 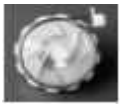 | 290g | 9 | 3500 | | Sleeve bearings (sintered slide bearings) and ball bearings (axial thrust bearing) | Lip seal | Microprocessor-based system controller<br><br>Reusable ultrasonic flow rate sensor | Open impeller with curved vanes<br><br>Activated by magnetic coupling | Clinical use (> 10 years) |
| RotaFlow  | 35cc | 10 | 4000 | | Magnetic stabilized rotor bearing (radial magnetic suspension)<br><br>Low friction blood-immersed pivot bearing --- sapphire ball ($Al_2O_3$) and polyethylene calotte without shaft seals | No seals | Flow and bubble sensors in drive unit, pressure transducers<br><br>Stand-alone console | Rotor powered by radial magnetic coupling<br><br>Logarithmic spiral channels | Clinical use |
| Nikkiso | 145g/25cc | 10 | 36000 | 15 | Ball bearings | V-shaped ring seal made of flurorubber | Ultrasonic flow meter<br><br>External console | Activated by magnetic coupling<br><br>Rotor driven | Clinical use |

| | | | | | | | | | |
|---|---|---|---|---|---|---|---|---|---|
| 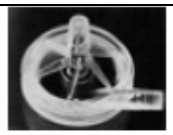 | | | | | | | | by console through flexible shaft<br><br>CFD studies on hemolysis<br><br>Six straight vanes, six washout holes<br><br>Two week with purging system washing the shaft-seal area<br><br>Joint venture: Baylor College of Medicine has lead to Gyropump | |
| HiFlow<br>  | 90g/30cc | 6 | 3500 | 25 | Spherical blood-immersed rotor thrust bearing . Ceramic-polymer bearing Minimal contact radius reduces heat generation within the bearing area | No seals | Pressure transducer and flow probe | Activated by magnetic coupling<br><br>Pulsatile pumping option | Laboratory |
| Rotodynamic<br>  | 207g/62cc | 5 | 3000 | 6-7 | Blood-lubricated hydrodynamic journal bearings<br><br>Magnetic attraction between stator-rotor acts as thrust bearing | No seals | Flow rate proportional to heart rate determined by pacemaker | Grooved bearing surface provides a self-pumping action that generates wash flow<br><br>Motor is surrounded by cooling blood flow<br><br>TETS used for energy supply | Laboratory |

| | | | | | | | | | |
|---|---|---|---|---|---|---|---|---|---|
| Gyro  | 305g/145 cc | 10 | 26000 | 7 | Duoble pivot bearing system at top and bottom of impeller Blood-immersed bearings<br><br>Alumina ceramic($Al_2O_3$) male pivot and polyethylene (UHMWPE) female pivot | No seals | Actuator controller | Eccentric inlet port eliminates obstacles in the blood path<br><br>Activated by magnetic coupling<br><br>GyroPI: Implantable-VAD GyroC1E3: Paracorporeal-CPB | Animal Expt |
| AB-180  | 284g/44c | 6 | 4500 | 4 | Bearings hydrodynamic journal bearing made of polycarbonate<br><br>Lubricated and cooled by sterile water/ heparin infusion | Polyurethane - coated rubber seal | Microprocessor-based device regulates pump speed, infusion rate and occluder safety system | Balloon occluder system: Prevents back flow from aorta to let atrium if the pump fails<br><br>Heparin infusion also used for anti-coagulation<br><br>Rotor is powered by electromagnetic coupling | Clinical use |
| Vienna 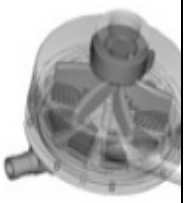 | 240g/101 cc | 6 | 2.5 | 15 | Hybrid mechanical-magnetic bearing system (permanent magnets)<br><br>Single mono-pivot mechanical support (ceramic/polyethylene) | No seal/shaft | Various controllers tested: Fuzzy non-linear and neuronal | Activated by magnetic coupling using double-disk motor<br><br>Magnets used both for driving and bearing | Animal Expt |
| Evaheart 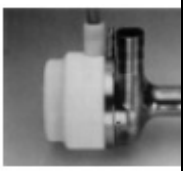 | 280g/150 cc | 7 | 2500 | 9-10 | Hydro dynamic journal bearing made of SiC<br><br>Lubricated and cooled by purge fluid (sterile pure water)<br><br>Viscous pumping effect by spiral grooves on bearing surface | Cool seal system: mechanical seal with circulating purge fluid | Ultrasonic flow measurement<br><br>Thermocouple meter for purge fluid temperature | Purge fluid continuously purified and sterilized by ultra filtration<br><br>Diamond-like carbon coating | Animal Expt |
| Abiomed CF | 190cc | 10 | 3500 | 25 (15 for beari | Active magnetic suspension in combination | No seals/shafts | Analog electronic feedback control | Activated by magnetic coupling using an | Laboratory |

| | | | | | | | | | |
|---|---|---|---|---|---|---|---|---|---|
|  | | | | ngs) | with hydrostatic stabilization<br><br>Electromagnets as actuators<br><br>Fluid between rotor and housing stabilize the magnetic suspension and contain axial motion | | system for radial position<br><br>Proximity sensors | internal motor<br><br>More compact and efficient system in future design | |
| Kriton<br>  | 195g/43cc | 6 | 5000 | 6-10 | Passive radial magnetic bearing acting in synergy with blood-lubricated hydrodynamic bearings eliminating the need for proximity sensors<br><br>Blood-lubricated pivot bearing to constrain axial motion | No seals | Pressure meter and transonic flow probes | Activated by magnetic coupling<br><br>Thick-bladed impeller due to imbedding of rotor magnets within the impeller blades | Laboratory |
| MSCP<br>  | 400g/196cc | 5 | 2 | 15 (9 for magnetic suspension) | Magnetic bearing<br><br>Magnetic suspension of impeller providing contact free rotation<br><br>Stainless steel motor bearings | No seals/shaft | Position sensors for magnetic suspension of bearings<br><br>Sensor less system: No need for a flow pro, flow rate obtained through motor current | Activated by magnetic coupling<br><br>Extracorporeal device available<br><br>Future design: TETS, pulsatile mode, implantable controller | Animal Expt |

Table 6: Detailed description of different types of Diagonal pumps [1]

| PUMP | WEIGHT/SIZE | FLOW RATE (L/MIN) | ROTATIONAL SPEED (RPM) | POWER REQ (WATTS) | TYPES OF BEARINGS | TYPES OF SEALS | TYPES OF SENSORS | ADDITIONAL FEATURES | STAGE OF DEVELOPMENT |
|---|---|---|---|---|---|---|---|---|---|
| VentrAssist  | | | | | Magnetic suspension coupled with hydrodynamic bearing<br><br>Fixed permanent magnets in upper and lower housing<br><br>Passively suspended rotor | No seals | External controller worn on belt<br><br>Sensor less motor control | Diagonal flow impeller activated by magnetic coupling<br><br>CAD and CFD optimized system<br><br>Vacuum-deposited coatings | Laboratory |
| HeartQuest  | 600g/275 cc | 10 | 2500 | 6.5 for bearings | Hybrid magnetic bearing: actuators are a combination of permanent magnets and electromagnets (reduced power consumption)<br><br>Full magnetic suspension | No seals/shaft | Sensor less system, controller monitors motor current and determines pump speed<br><br>Position sensors for bearings | Mixed flow impeller<br><br>Motor integrated into the pump impeller and stator<br><br>QuestCoat: flexible ceramic coating | Laboratory |
| DeltaStream  | 300g/150 cc | 8 | 9000 | 40 | Ball bearings located inside the motor chamber | Lip seal (polyurethane) | Ultrasonic flow probe<br><br>Hall sensor for motor speed<br><br>Humidity sensor inside motor<br><br>Temperature sensor on motor housing<br><br>External console | Pulsatile flow option<br><br>CFD studies<br><br>Highly integrated design | Animal Expt |

Table 1 is the list of axial pumps available in the market where as table 3 describes three type of diagonal pumps that are available with their developers name. The axial blood pumps, centrifugal and diagonal pumps further charted into a table with more detailed format of their power requirements, type of sensors, rotational speed etc. This table of detailed data can be referred from tables 4, 5 and 6 [1] and can be used as literary reference for the study of different axial and centrifugal pumps.

**1.1. Need for improved design:**

With all the technological advance and availability of different tools for proper pump design, it is still important to build, test and then improve any design. Due to variable nature of the blood, it is very essential to build and test the pump design accurately. Despite of all these, rotary pumps have their own hazards such as shear rate compensation. Rotary pumps are best to obtain high flow rates, nearly 20L/min [1] but despite of all advantages, these pumps has limitations over the cavitations threshold and maximum allowable shear rates.

Hemolysis and platelet activation are affected by both shear stress and transition time in the pump [2]. In addition, blood trauma and blood cell destruction are most common. During the sealing, the heat generation also leads to local thrombus formation. These factors increase the risk of patient's life and also call for the need of technical solutions with improved quality of life. One of the major causes of death in USA is the Low output syndrome (LOS) after an open heart surgery. In addition to post- operational low output, cardiogenic shock or cardiac fibrillation also demands for more efficient means of cardiac assistive devices.

To avoid and reduce these causes due to traditional pumps, a pulsatile-continuous flow pump design is considered [13]. The main aim of the pump is to provide a 20% cardiac assist to a person with congestive heart failures and other cardiac diseases. The pump under development is designed by utilizing a unique geometry and pumping actuation mechanism which helps to maintain low blood trauma, low anticoagulation levels preventing thrombosis and thus, less hemorrhage chances. This design also uses polyethylene oxide (PEO), a biocompatible material, which minimizes the protein interaction with the interior pumping surface thus reduces the coagulation of blood due to interaction.

The design utilizes biocompatible material, Polyethylene oxide (PEO), which minimized protein interaction with the interior pumping surface. Shape memory alloy actuators compress the pumping chamber. Shape memory alloy actuators also actuate compression of the ingoing sphincter valve and outgoing sphincter valves. Pumping motion can be analyzed by accelerometers to provide optimized feedback and pump motion control.

# CHAPTER 2

# BLOOD RHEOLOGY

The main concern of the project is to develop a design which can overcome the problems caused by the conventional pumps in the market. One of such problems is the hemolysis: the destruction of red blood cells causing the release of hemoglobin to the blood plasma. Hemolysis leads to platelet activation and thereby results in blood coagulation. Device induced platelet activation also leads to the consumption of anticoagulant drugs by the patient which over a period can cause internal bleeding. To help build an efficient design, one has to understand the fluid properties of blood.

When compared to water, blood is acts as a non-Newtonian fluid. The study of blood fluid dynamics has been carried out from a very long period to better understand the flow in arterial, venal and extracorporeal systems. Extensive study of the flow pattern and deformation of blood components is known as rheology. The deformation in case of blood refers to the viscoelastic behavior of blood.

As described earlier in chapter 1, most of the disadvantages of the current pumps lies in the vast abnormality of blood pattern. To get a pump to work without major drawbacks, one has to understand the components involved in the blood flow dynamics. The major factors affecting are blood plasma viscosity, RBCs (Red Blood Cells), WBCs (White Blood Cells), platelets, the hematocrit value of blood, fibrinogen and temperature.

## 2.1. Blood behavoir:

Two study the fluid flow pattern of a blood we have to first understand the two main groups of liquid which are classified on the basis of viscosity and shear rate or

shear stress. First is Newtonian fluids in which viscosity is independent of the shear rate. Second is the non-Newtonian fluid in which viscosity may increase or decrease based on the shear rate. The magnitude of viscosity is calculated as the ratio of shear rate to shear stress. Shear stress is defined as the ratio of shear force to area.

Shear stress $T = F/A$ (dyne/cm$^2$)

In the study of fluid mechanics for a pipe with constant diameter and length, the resistance to flow depends on the flow conditions within the pipe. If the flow of fluid is slow then the pressure drop is proportional to the flow velocity. In this case the fluid particles move smoothly and parallel to the tube wall. Such a type of flow is called as laminar flow. On the contrary when the pressure drop in the tube is proportional to the square of the flow speed then the flow pattern is called turbulent which is a more chaotic form of flow. The resistance to flow is more in turbulent pattern when compared with the laminar flow.

**2.2. Newtonian and non- Newtonian Fluid:**

As discussed earlier Newtonian and non-Newtonian fluids are the two classification of fluids which are based on the independency and dependency of viscosity on shear stress and shear rate respectively. In non-Newtonian fluids, the viscosity either increases or decreases with the increase in shear rate. As shown in figure 3 for Newtonian fluid, the slope of a shear stress versus shear rate graph gives a constant viscosity whereas for non-Newtonian fluid it varies along the graph. Non-Newtonian fluids have yield stress below which the shear stress is finite and the shear rate is zero giving an infinite viscosity condition. In case of blood if the yield stress is exceeded then the deformation of blood cells is irreversible leading to thrombosis.

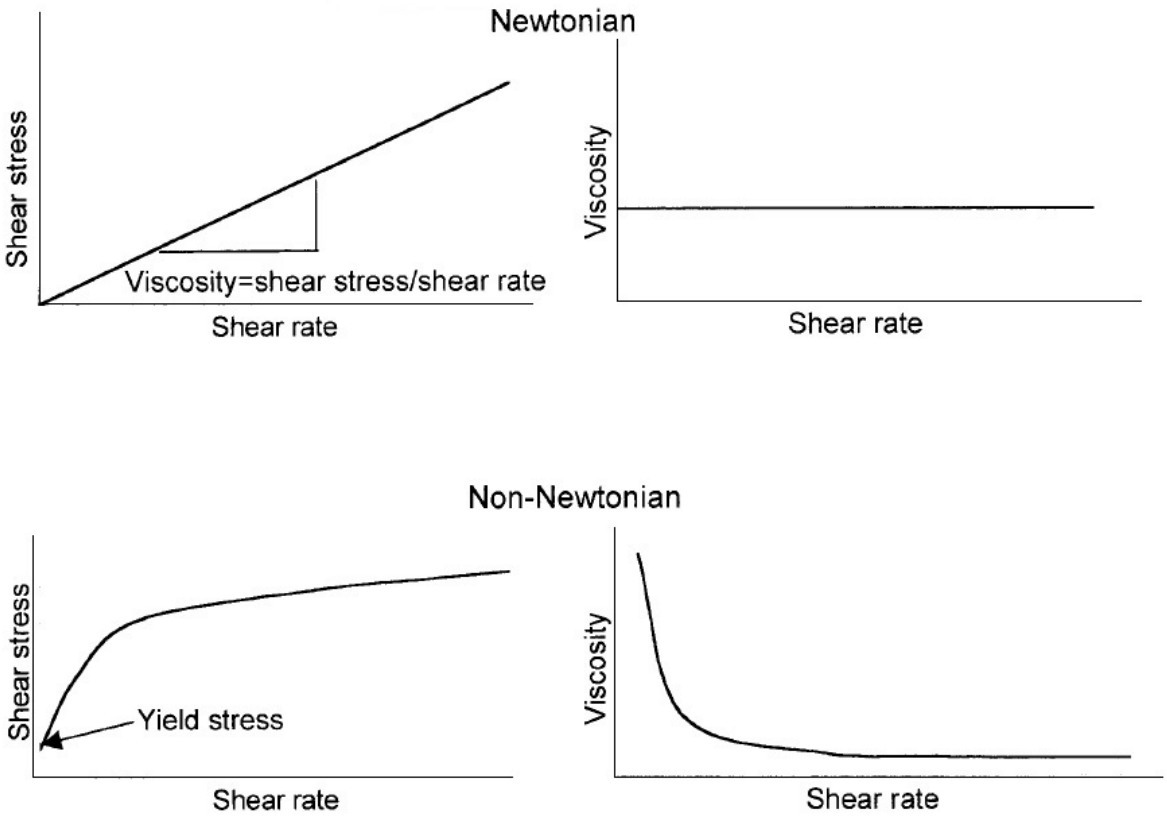


Figure 3: Shear stress and shear rate relationship in Newtonian and non-Newtonian fluids

If the viscosity decreases with increase in shear rate, then the fluid is called shear-thinning fluid and if the viscosity increases with the increase in shear rate then it is called shear- thickening. Human blood behaves as a shear-thinning fluid with viscosity varying between 4 to 5 centipoise (cP) at 37$^{o}$C when observed at high shear rate of 100 to 200 sec$^{-1}$. With further increase in shear rate, viscosity becomes insensitive to shear rate. When the shear rate is reduced below 100 sec$^{-1}$, viscosity increases exponentially with decrease in the shear rate.

The coefficient of viscosity, $\eta$, in fluid mechanics is given by the ratio of shear stress T to shear strain rate $\dot{\gamma}$ (also called velocity gradient):

$$\eta = T/\dot{\gamma} \text{ (dynes-sec)/cm}^2\text{(poise)}$$

The steady state laminar flow can be given by Poiseuille's equation for a straight cylindrical tube:

$Q = \pi * \Delta P * R^4 / L * 8\eta$ where Q is the flow rate, $\Delta P$ is pressure difference, L is the length of the tube , R is the inner radius of the tube. This equation leads to the conclusion that for Newtonian fluids if the viscosity is doubled, the flow rate can be reduced to half and if the radius of the tube is doubled, it will lead to a 16 fold increase in the flow rate.

To experimentally measure the fluid viscosity of Newtonian fluids capillary viscometer is used, whereas to measure non-Newtonian fluid this instrument is not enough. Hence Couette viscometer , cone-in-cone viscometer or cone-on-plate viscometer is used. Despite of all these it is still difficult to study the rheology of human blood.

A small experiment where human blood was induced with ACD (anticoagulant citrate dextrose) solution a particular relationship between shear stress to shear strain rate was found which later developed as Casson's plot [11] as shown in figure 4 [8]. Casson's plot is also known as the double square root plot. It became apparent from these plots that blood behaves non-Newtonian near the origin implying that below 100 $sec^{-1}$ shear strain rate it obeys the non-Newtonian regime and after certain rate above that it obeys Newtonian regime. The Casson's plot curves derives the following relationship between shear stress (T) and yield stress ($T_y$):

0-20 $sec^{-1}$: $T^{1/2} = T_y^{1/2} + \eta_N^{1/2} \dot{\gamma}^{1/2}$

above 100$sec^{-1}$: $T^{1/2} = \eta_N^{1/2} \dot{\gamma}^{1/2}$ or $T = \eta_N \dot{\gamma}$ where $\eta_N$ is the ultimate Newtonian viscosity and $\dot{\gamma}$ is the shear strain rate. Hence blood exhibits a viscoelastic behavior with the non-Newtonian property more dominating.

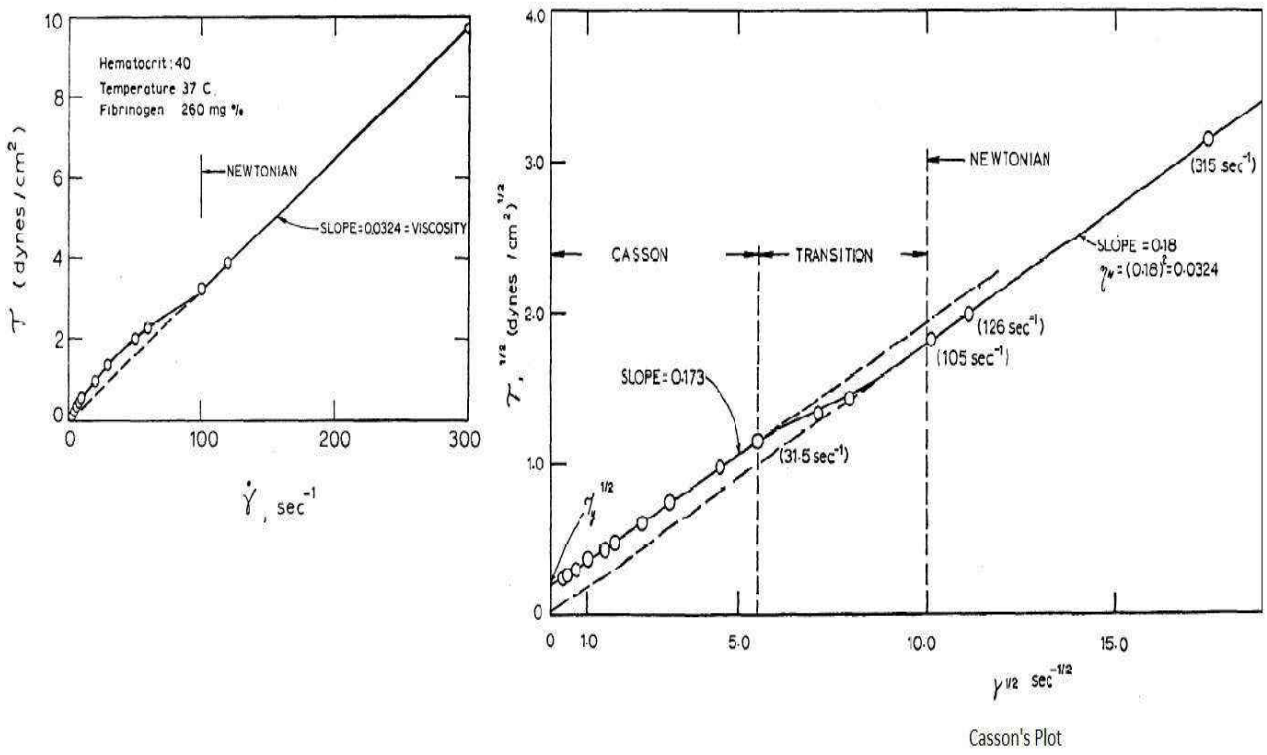


Figure 4: Non- Newtonian shear stress and shear strain rate along with Casson's Plot [8]

### 2.3. Blood components:

#### 2.3.1. Blood plasma:

Plasma is the suspension portion of the blood which contains the RBCs, WBCs and platelets along with other proteins and salts. The normal range of blood plasma viscosity varies between 1.10 and 1.35 centipoise(cP) [6], [7]. The change in plasma viscosity directly affects the blood viscosity value. This change is irrelevant to the hematocrit value and the other cellular elements. Studies have shown that plasma acts as a Newtonian fluid but the presence of elements in it makes it to behave as non- Newtonian.

#### 2.3.2. RBC aggregation and deformation:

The pattern of flow streamlines depend on the concentration of RBCs and the deformation of these cells under pressure, specifically shear forces. RBCs affects the flow of

blood in a vessel by either subjecting itself to sedimentation against gravity or the densification process thereby increasing the hematocrit value[9].

Healthy RBCs easily responds to applied forces and gets deformed with changes in their shape. RBCs have biconcave disk shape which also behave as elastic bodies. Generally the deformation is reversible but in cases of increased shear rate, the change happens for permanently. Due to the shape change and applied pressure, the RBCs aggregate to form linear arrays in the form of stack of coins, termed as rouleaux. These further aggregate to form 3D structures. The aggregate formation increases the blood viscosity to a great extent.

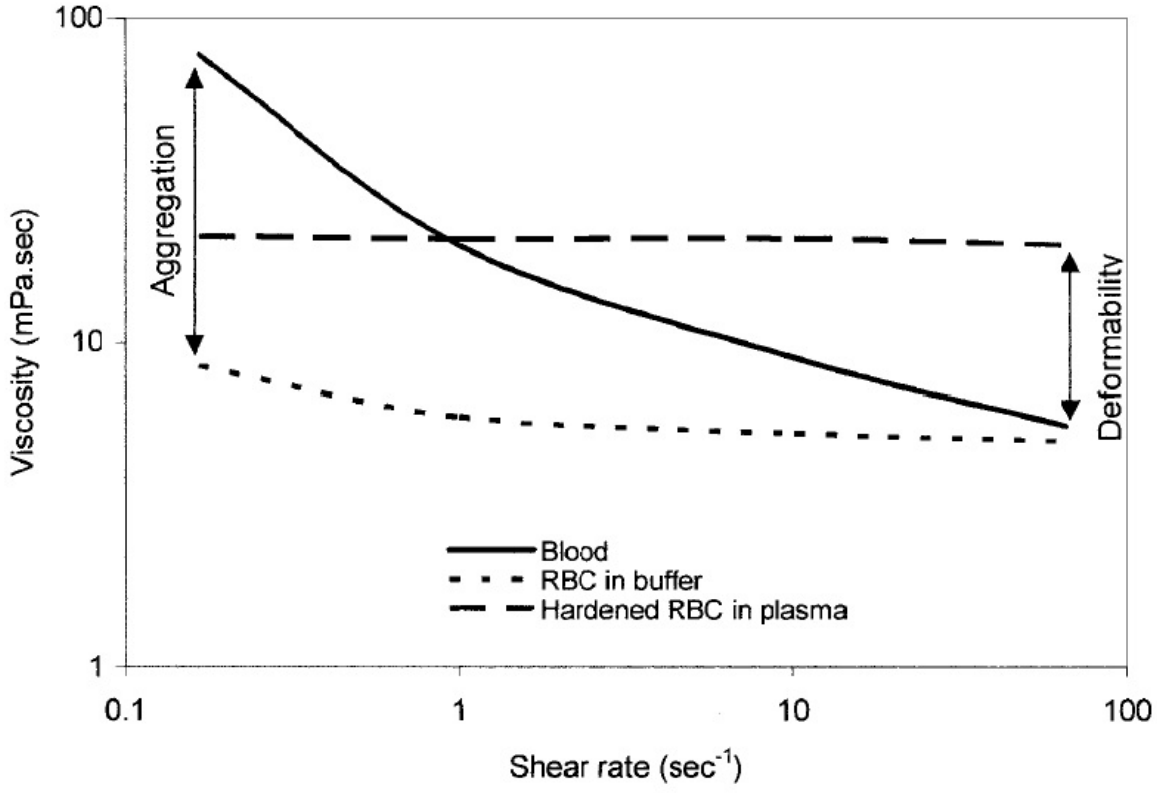


Figure 5: Relationship between the viscosity of blood and the shear rate [6]

Within normal blood parameters, the aggregation process is in balance with disaggregating forces. An increase in the shear rate disintegrate the aggregates and a reduction the shear rate would increase the aggregate formation(9). Figure 5[6] gives an overview of the aggregation and deformation curve with applied shear rate.

**2.3.3. Hematocrit:**

Hematocrit is the value which gives the measure of red blood cells in the blood by percentage volume. It defines the packed RBC cell volume. This value varies differently for men and women from a range of 40.7 -50.3 %, 36.1-44.3%, respectively. Figure 6 [1] [6] shows the correlation between the viscosity and the hematocrit value of blood.

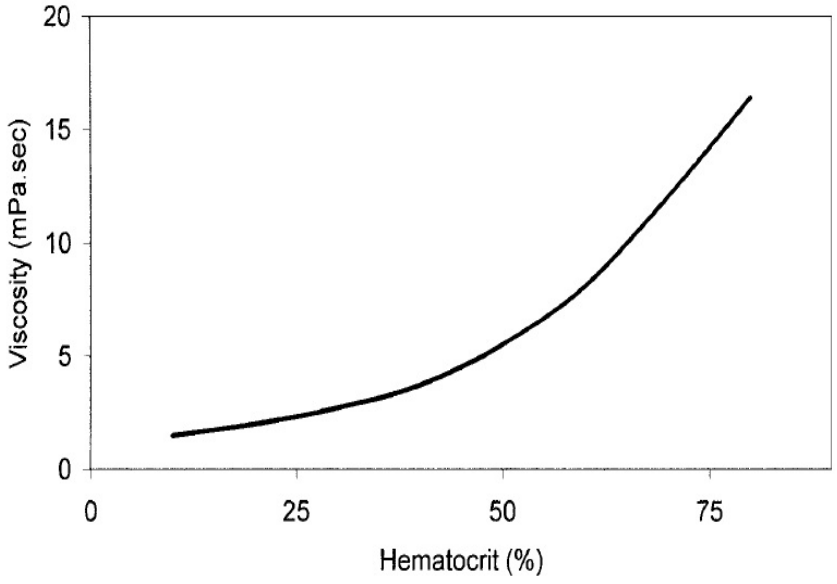


Figure 6: Graph showing relationship between blood viscosity and hematocrit value. [1] [6]

It can be observed from figure 6 [1] [6] that there is an exponential increase in the value of viscosity with an increase in the hematocrit value. There is an increase of 4% in blood viscosity for a unit increase of hematocrit at medium to high shear rates. The relation between hematocrit H and plasma viscosity $\eta_p$ can be given as

$\eta_N = \eta_p \{ 1+ 0.025H + 7.35 * 10^{-4} H^2\}$ where $\eta_N$ is the ultimate Newtonian viscosity over a range of $\eta_N$ ranging from 0.03 P at hematocrit of 40 to 0.10 at hematocrit 65 [8] .

For non- Newtonian regime, the yield stress ($T_y$) is best correlated with hematocrit over a range to 30-50 with the following equation:

$T_y = A (H-H_c)^3$ where A is constant ranging between 0.6-1.2 * $10^{-6}$ and $H_c$ is the limiting hematocrit between 4 and 8. The value of A is highly dependent on the fibrinogen concentration. At a hematocrit of 40 the yield stress value is typically 0.04 dyne/$cm^2$. With an increase in the hematocrit value above 50, the blood displays various rheological abnormalities.

**2.3.4. Fibrinogen:**

As stated above the fibrinogen concentration plays a major role in the blood viscosity determination. The fluid pattern of blood heavily depends on the red blood cell and fibrinogen interaction. The variation of yield stress $T_y$ and fibrinogen concentration $C_f$ can be given by the equation

$T_y = B C_f^2$

where B is a constant varying between 1 * $10^{-11}$ to 2 * $10^{-11}$ and weakly depends on the concentration of other proteins in the blood plasma. This equation is valid over a range of 100-400 mg% concentration of fibrinogen [8].

**2.3.5. Temperature:**

When blood follows the range of Newtonian fluid, it is observed that the temperature coefficient of viscosity is same as that of water over a range of 10-37 C [10]. In the non-Newtonian range , the viscosity and fluid flow are less affected by the temperature.

For 90% of human subjects the yield stress was independent of temperature but for the rest of 1% there was a small increase in the yield stress with a decrease in the temperature.

**2.3.6. WBCs and Platelets:**

Generally WBCs and platelets does not contribute to the macroscopic fluid properties of blood due to the less concentration of these components as compared to the RBCs present. These although influence the blood flow resistance in microcirculation.

**2.3.7. Thrombosis:**

Thrombosis in general terms is the clotting of blood. Blood clotting in the pumps is a major factor of pump failure. Thrombosis happens as a result of red blood cell aggregation at high shear rates which induces the activation of platelets and fibrin forming first a mesh like structure leading to the clot formation. Thrombosis results in the increase in the blood viscosity which in some cases leads to clotting of remaining blood in contact.

**2.4. Effect of fluid mechanics on pump development:**

While design the pump we have to keep in consideration the semi Newtonian and non-Newtonian fluid pattern of the blood along with all the above mentioned factors affecting the viscosity of blood. Since the pump acts on the arterial blood pressure, the flow velocity becomes sufficiently high indicating that the shear stress corresponds to the Newtonian part of the blood fluid dynamics. The viscosity of blood flowing through tubes having smaller diameter reduces and as the diameter decreases further, the viscosity value increases sharply.

Also the hematocrit value of blood inside the tube is less and the hematocrit value at the discharge outlet i.e., at outflow is more. During the flow of blood through a vessel two major factors affect the blood viscosity thereby leading to clot formation: a) the

sedimentation of red blood cells due to effect of gravity to the vessel lining, b) when in vertical position due to axial movement of red blood cells in the vessel, flow resistance is reduced leading to low viscous regions near the tubes of the vessel wall. Hence blood flow velocity and pumping efficiency depends on the aggregation and deformability capacity of red blood cells, sedimentation property due to orientation of pump and gravity, tube diameter, fibrinogen to fibrin formation.

Also lysed red blood cells, free hemoglobin in plasma and presence of air bubbles affects the pump function. Lysed red blood cells comes in contact with healthy cells and thereby activates fibrinogen forming aggregates of these lysed (ghost) cells. If the free hemoglobin concentration in the plasma increases then it results in the increase of yield stress. The chance of developing air bubbles in the pump can have a lethal impact on the person as it leads to hemolysis: the breaking of red blood cells releasing the hemoglobin into blood plasma which induces a reaction chain of thrombosis and embolization (formation and circulation of embolus, an intravascular mass) . Understanding these factors help in the development of a better pulsatile pump although in-depth apprehension of blood rheology still needs to be carried out.

# CHAPTER 3

# DESIGN PRINCIPLE AND WORKING

## 3.1. Design:

As discussed in the previous chapters the major hurdle in the development of the pump is to design a model which can minimize the shear stress and therby can reduce the blood cell damage it causes. To achieve such a design different design prototypes were considered with extensive research and one working design is proposed which considers the principle of a low shear pump and utilizes a unique geometry and pumping actuation mechanism.

The proposed working prototype of the pump was created using AutoCAD. The following figures shows the front view and side views of the pump.

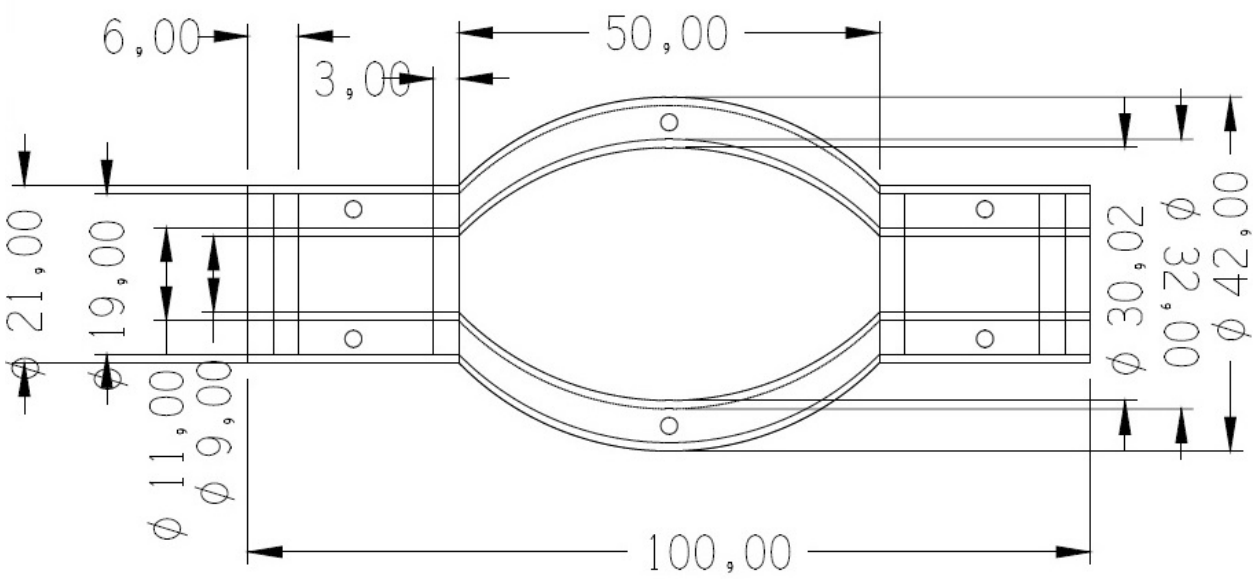


Figure 7: Front view of the proposed pump

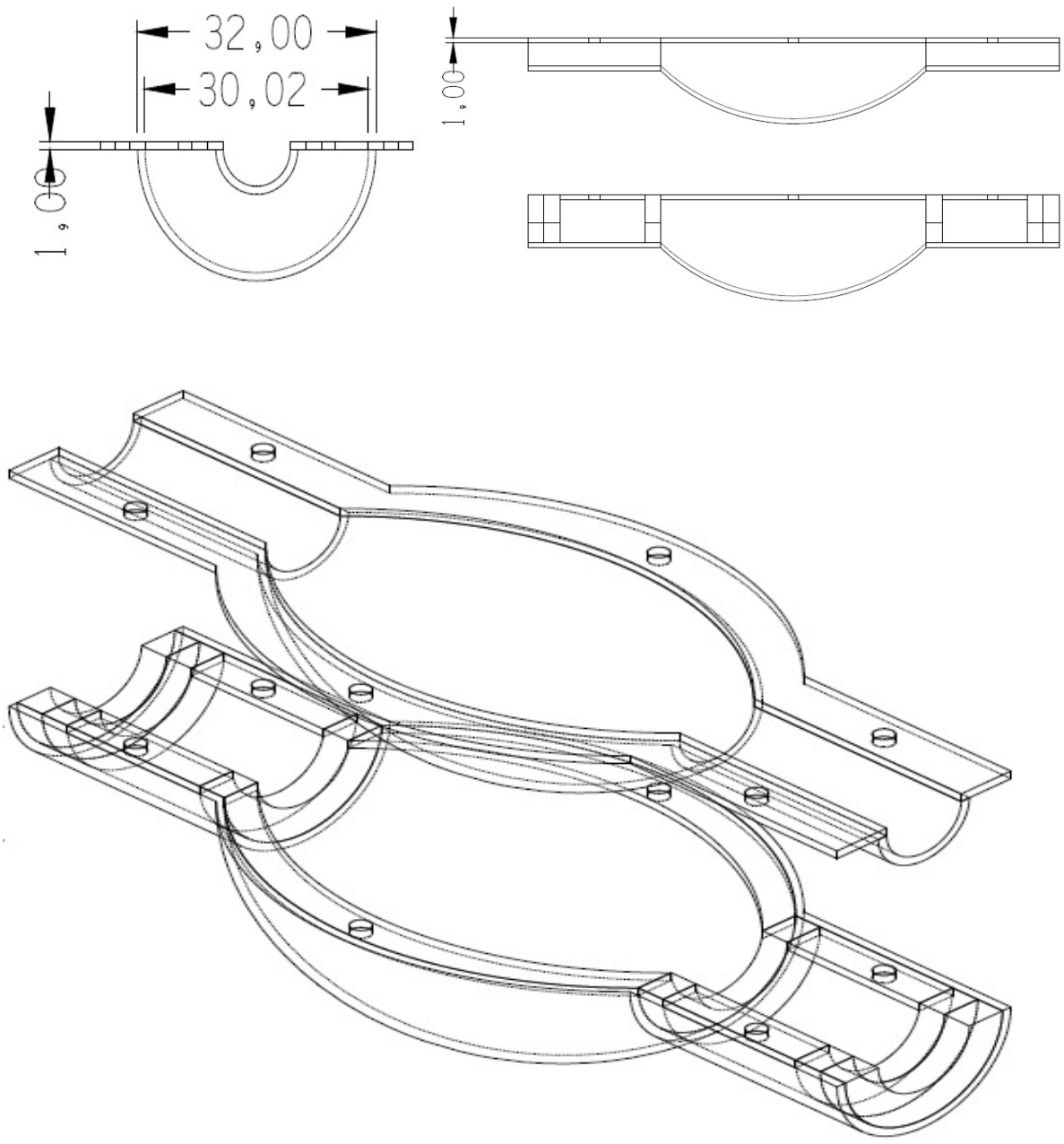


Figure 8: Side views of the pump design.

To validate the two dimensional design, we needed to study the volume covered inside the tube, flow obtained and which pattern of flow is observed. To understand the volume contained by our design mathematical calculations can be used. The pump design can be approximated to the combination of two cylinders with an ellipsoid. Now the

total volume contained inside the pump will be the addition of volume of two cylinders and the volume of ellipsoid.

Volume of pump= 2* volume of cylinder + volume of ellipsoid

$= 2 * \pi*(4.5)^2(25)+ 4/3* \pi* 50/2*30.2/2*30.2/2$

$= 2* 1590.43 + 23865.0467 \ mm^3$

$= 2 * 1.59 + 23.86 \ cm^3$ (approx)

$= 27.04 \ cm^3$ (approx)

Now this implies 0.027 liters per sec . So the per minute output will be $(1.59+23.86)cm^3 * 60$ minute. this can be equated to :

Volume flow out = $25.45cm^3$ *60/ minute

= .02545*60 L/min

= 1.527 L/min (approx)

So this falls under the proposed domain of the output that the design produces. Also to validate the design technical aspects and to check whether the design produces a flow patter in the laminar flow range we calculated the Reynolds number at the output of the pump. In general, Reynolds number = $\rho QD/ \mu A$ where $\rho$ is the density of blood (1060 $kg/m^3$), Q is the flow rate, D is the diameter of the tube, $\mu$ is the dynamic viscosity of blood ($3.5*10^{-3}$ Pa.s) and A is the cross sectional area of the tube.

Reynolds number= $(1060*25.45*10^{-6}*0.009)/ 3.5*10^{-3}*\pi*0.009(4.5+25)*10^{-3}$

= 83.2 (approx) , showing that the flow obtained at the end is a laminar flow.

A three dimensional figure of the model was created which shows the pump as a whole with its input and output outlets. Figure 9 shows the 3D picture depicting the

sphincters and valves of the pump. Figure 10 and figure 11 shows the two dimensional cut section and the layer section of the pump.

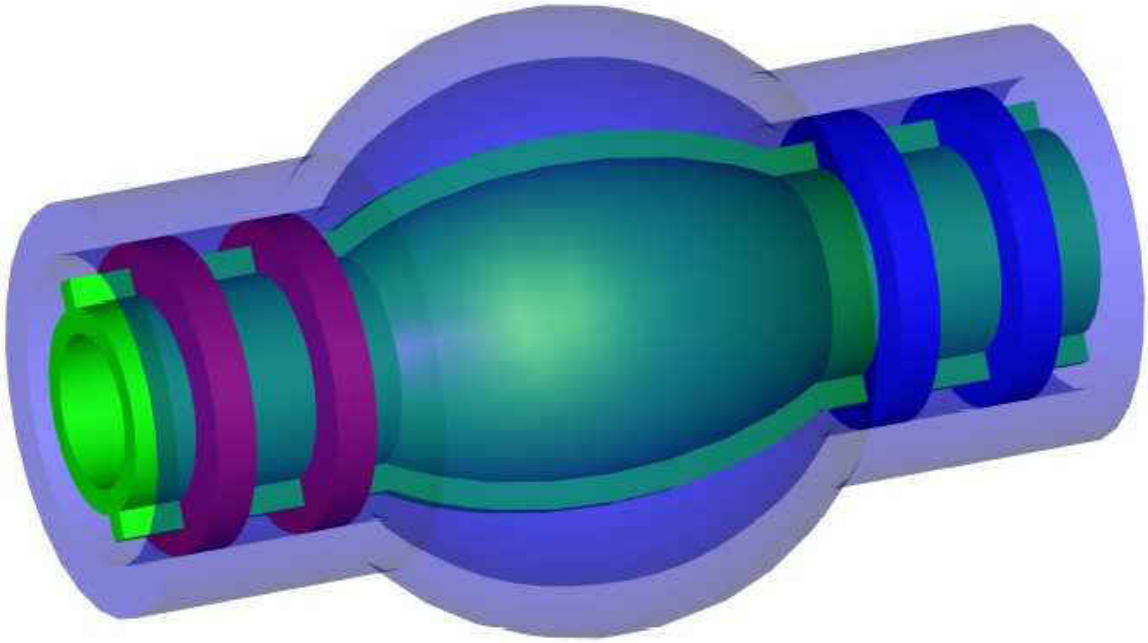

Figure 9 : Three dimensional model of the proposed pump

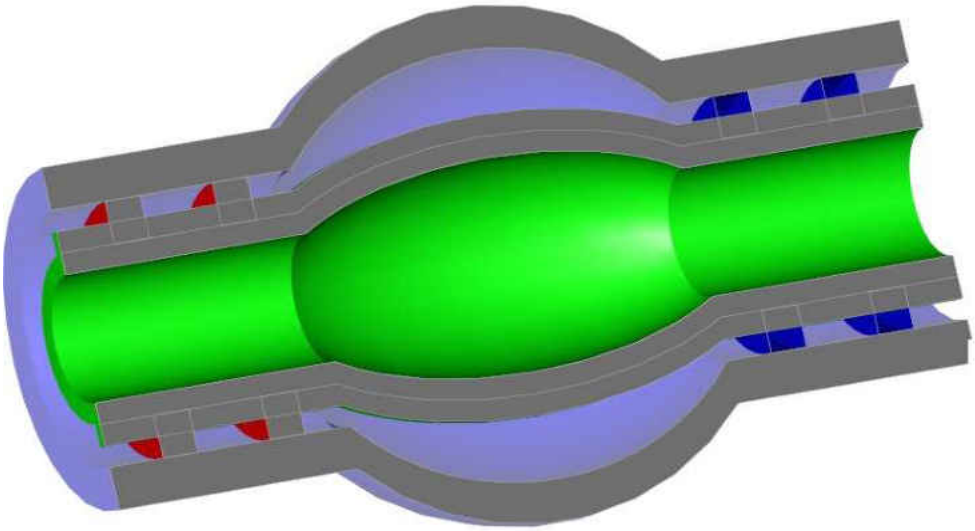

Figure 10: The two dimensional cut section

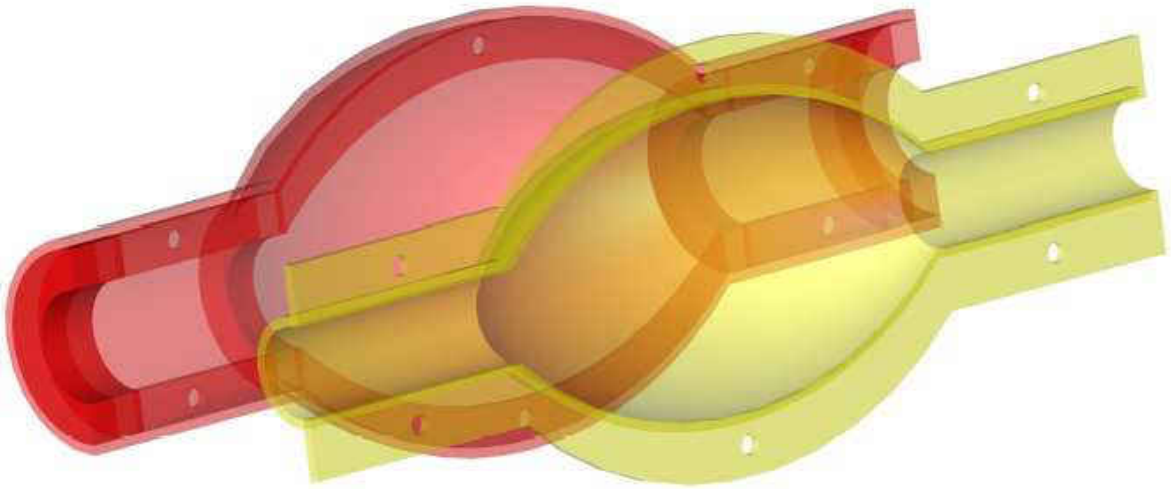

Figure 11: Layer section of the pump

After the two dimensional and three dimensional design manifestation, to aid this design the flow dynamics of the model is studied using COMSOL simulation.

**3.2. Principle:**

The design and working principle of the pump are developed by considering all the major factors affecting the current pumping and assistive systems. The main principle involved in the design of the pump is the implementation of the pulsatile motion into the pump which biomimics the actual heart compression and pulsation. The duty of the pump is to provide assistance to a weak pumping heart. After studying the arterial pressure and cardiac output of the heart, the blood flow was stated according to the Darcy's Law of calculating Mean Arterial Pressure (MAP). According to this law :

$$MAP = CO*SVR + CVP$$

where CO is cardiac output, SVR is systemic vascular resistance, CVP is central venous pressure. This equation can be simplified as $MAP \sim P_{dias} + 1/3 * (P_{sys} - P_{dias})$, where $P_{dias}$ is diastolic pressure and $P_{sys}$ is the systolic pressure. For patients having low

pumping pressure and to increase the blood pressure, the pump would provide an increase of 20% to blood pressure by pumping the blood from the venous supply to the arterial supply as seen from figure 12. For this purpose the blood pumping flow rate should reach the 20% of the normal rate, which make the proposed pump to produce a flow rate in between 1L/min to 2L/min.

As discussed in the earlier chapter the high speed rotation pumps and displacement pumps produces high shear stress which cause blood thrombosis and embolization. So the pump design has to be a prototype which causes low blood damage and to achieve this, pulsatile pumping motion mimicking the actual heart compression and decompression process is used.

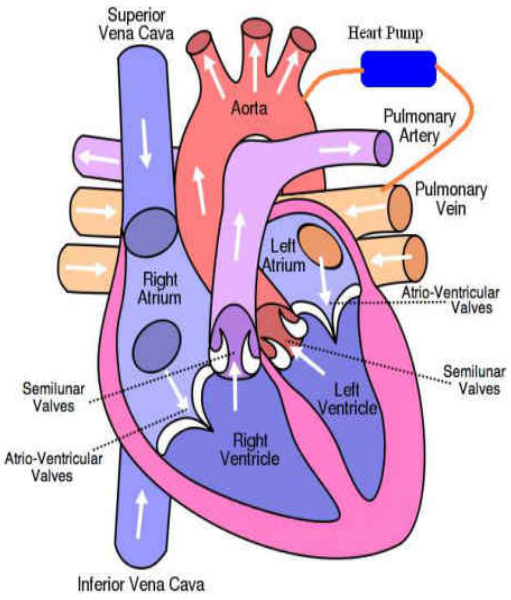


Figure 12: Proposed positioning of the pump in development.

The pump has a minimum pressure capacity of 120 mmHg at 50 to 150 heart beats per minute. Since the pump design provides 50 to 120 beats/minute, the average number of times it beats per minute can be calculated as: 50+120/2=85 beats (average)/min.

Therefore, time taken for one beat will be: 60/85= 0.7058 sec approximately. Process of compression and decompression relates to one complete cycle of pump. So compression and decompression takes half of the pump cycle respectively. Therefore time taken to compress could be approximated as 0.7058/2= 0.3529 sec. Similarly the time taken to decompress also approximates to 0.3529 sec. This pressure can be measured using blood pressure sensors or direct electro cardiac sensing. This pumping principle provides a wide variety of applications not just limited to the arterial pumping.

**3.3 Working Mechanism:**

As described in the principle, the proposed pump works on the pulsatile compression an d decompression mechanism of the heart. The design follows unique geometry where we first study the flow and fluid dynamics using simulation techniques. The proposed theory of pump can use shape memory alloy actuators which helps in the compression of the pumping chamber. Also pneumatic cuffs can be used to inflate and deflate the pump body. These cuffs also control the compression of the sphincters attached at the input and the output which are used to minimize the thrombosis caused by turbulence. Although shape memory actuators can also be used, the design with pneumatic cuffs has been studied as it helps simple sequencing of the two-way valve.

Figure 13 shows the prototype model using the pneumatic cuffs for the compression and decompression of the pump. The pump follows a basic mechanism: as the blood flows in through the input, the input valve opens creating the pump chamber to inflate and then as soon the chamber fills in, pressure builds up causing the input valve to close and the output valve opens which thereby results in the compression of the pump and output flow of blood. To achieve sequential actuation of complex and continuous flow pattern in the

pump, a cluster of pumps (each independently controlled) can be packaged together with low turbulence flow. This type of zonal compression allows optimal compression for blood flow.

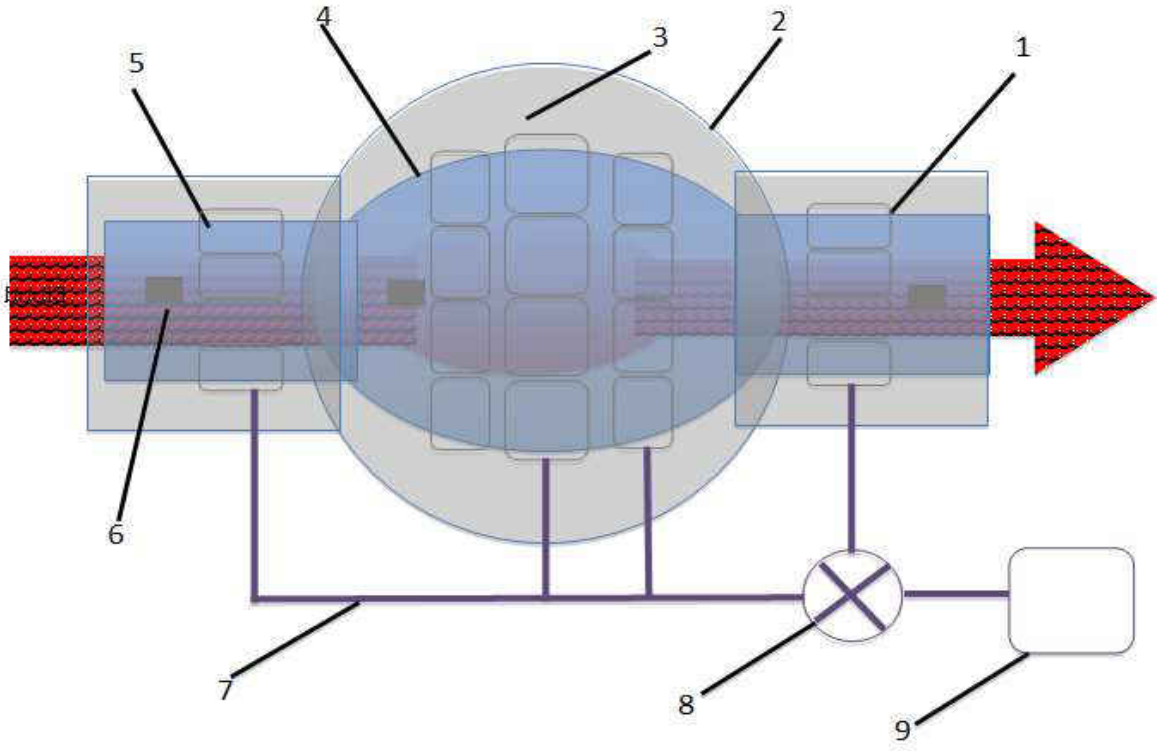


Figure 13 : A pneumatic version of the pumping apprentice. (1) outgoing sphincter valve controlled by pneumatic cuff, outer titanium case, (3) main pump pneumatic cuff actuator, (4) polymer pump body with PEO lining, (5) inlet sphincter valve cuff, (6) 6-axis accelerometer chips for actuation analysis, (7) pneumatic control lines, (8) valve to control actuation, (9) pneumatic pump (saline or gas).

**3.4. Simulation:**

As described earlier, to fully understand the mechanism of fluid flow of the proposed pump design and to aid the design development, the simulation study of the pump is conducted through COMSOL multiphysics software. To better understand the fluid flow properties a peristaltic model is stimulated which can help understand the stress applied on the fluid and to observe the velocity field of the flow in the pump.

In the developed model, the flow of fluid is through a cylindrical pipe and external pressure is applied which leads to the deformation of the tube thereby creating stress in the fluid. The simulation consist of transient analysis based on incompressible Navier-Stokes equation which is given by

$$\rho\frac{\partial \mathbf{u}}{\partial t} - \nabla \cdot \eta(\nabla \mathbf{u} + (\nabla \mathbf{u})^T) + \rho \mathbf{u} \cdot \nabla \mathbf{u} + \nabla p = 0$$

$$\nabla \cdot \mathbf{u} = 0$$

where $\rho$ is density (kg/m$^3$), $\mathbf{u}$ is flow velocity (m/s), η is viscosity (Pa.s) and p is pressure. The model uses simple geometric construction of a rectangle to model a cylinder as seen from figure 14 and has a set of constants tabulated in table 2.

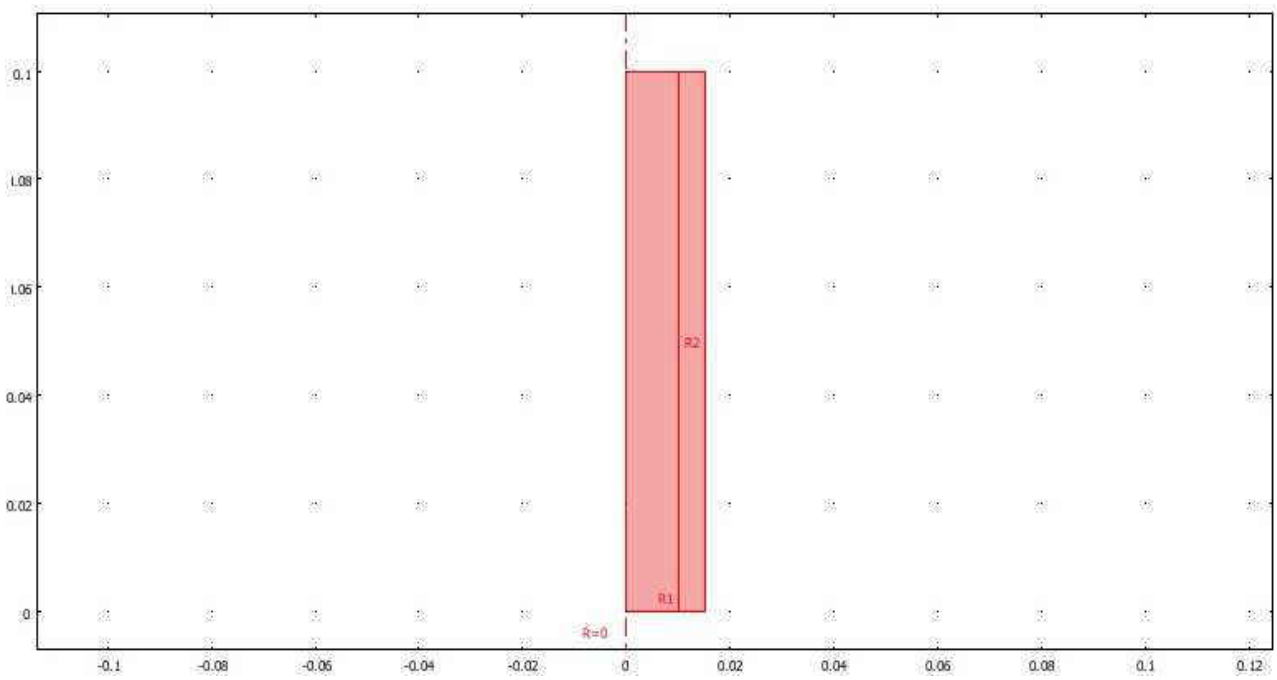


Figure 14: Geometric model construction

The model use three application modes: axial symmetry, stress-strain ; moving mesh and incompressible Navier- Stokes system. Hence this model becomes a combination of structural mechanics and fluid dynamics. The moving mesh application is used to study the deforming geometry of the model.

| Name | Expression | Value | Description |
|---|---|---|---|
| t_on | 0.3[s] | | Time when roll is engaged |
| t_off | 1.2[s] | | Time when roll is disengaged |
| dt | 0.2[s] | | Time to reach full force |
| z0 | 0.03[m] | | z coordinate where roll starts |
| v0 | 0.03[m/s] | | Vertical velocity of roll |
| width | 0.01[m] | | Width of Gaussian force distribution |
| Ttot | 1.5[s] | | Total time for a pump cycle |
| Lmax | 4e6[N/m^2] | | Max load |

Table 7: Set of Constants used for modeling

For developing the fluid simulation, the boundary conditions at the inlet and outlet of the pump assumes that :

$$\mathbf{n} \cdot [-pI + \eta(\nabla \mathbf{u} + (\nabla \mathbf{u})^T)] = \mathbf{0}$$

This implies that the total stress at the inlet and the outlet of the pump is zero. While configuring the moving mesh, it is fixed to a zero *r* displacement at the symmetry axis and at the top and bottom of the tube it is at a zero *z* displacement. To obtain the volumetric flow rate ( $\dot{V}$ ) in $m^3/s$ at the input and output is given by

$$\dot{V}_{\text{in}} = -\int_{s_{\text{in}}} 2\pi r(\mathbf{n} \cdot \mathbf{u}) ds$$

$$\dot{V}_{\text{out}} = \int_{s_{\text{out}}} 2\pi r(\mathbf{n} \cdot \mathbf{u}) ds$$

where **n** is the outward-pointing unit normal and s is the boundary length parameter. Similarly the total volume of the fluid in $m^3$ can be calculated using

$$V = \int_A 2\pi r dA \qquad V_{pump}(t) = \int_0^t \dot{V}_{out}\, dt$$

$$\frac{dV_{pump}}{dt} = \dot{V}_{out}$$

where A is the deformed domain. $V_{pump}$ is the volume of fluid that comes out through the outlet. The derivative equation is then used to derive the above stated integral. The boundary conditions for the model are set accordingly and a major equation is used to set the edge load i.e. the load or the decompression on the pump. The load acting is force per unit area with a boundary setting of {-Lmax*flc2hs((t-t_on)[1/s], dt[1/s])*gauss((z-0.05)[1/m],width[1/m])*flc2hs((t_off-t)[1/s],dt[1/s])} where the middle factor plays a major role in the positioning of the pressure. In the simulation we apply the load at the midpoint of the tube.

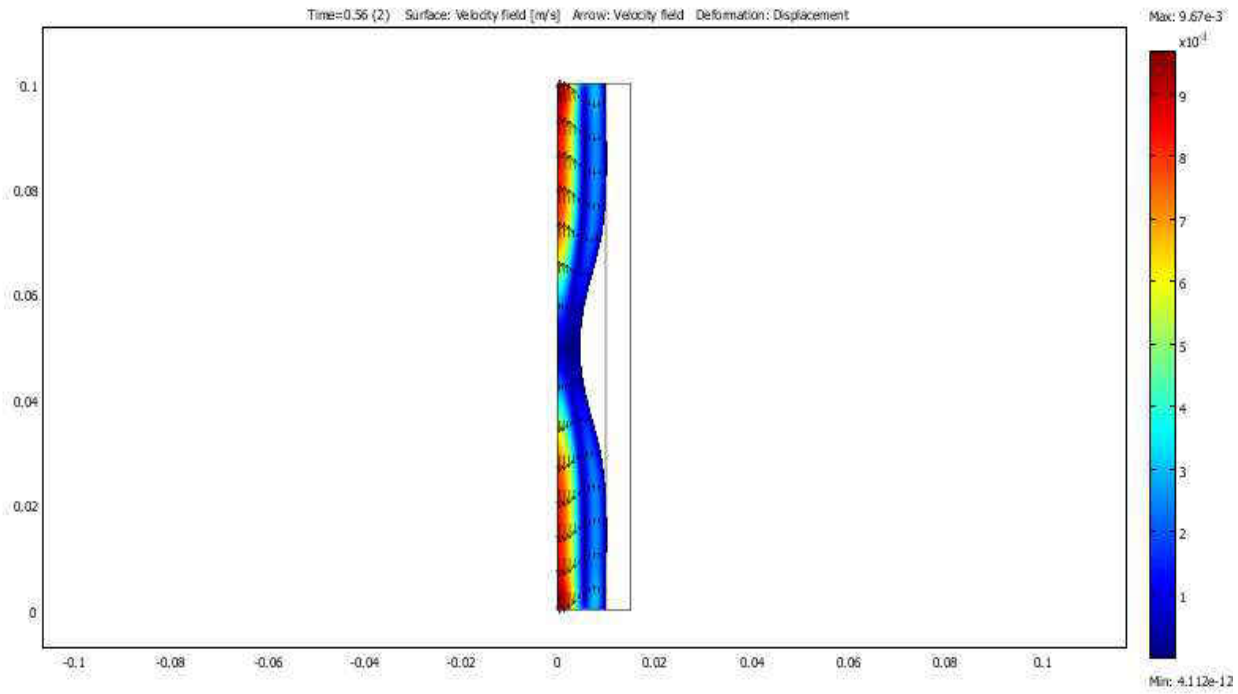


Figure 15: End result of simulation depicting the load applied

Figure 15 shows the end result of the simulation with the velocity - deformation profile. A full detailed report of the simulation with all the tables and boundary conditions are provided in Appendix 2.

# CHAPTER 4

# MATERIAL USED

The material used to develop the inner sheathing of the pump is implant grade liquid silicone rubber (LSR). Liquid silicone rubber is a curated silicone with high purity platinum at low compression set properties which has more stability towards extreme temperature variation from hot to cold and can also be molded into various wall thickness within a same part - a requirement for the production of high quality parts.

## 4.1. Chemical background and uses:

Liquid silicone rubber belongs to a family of thermoset elastomers with a chemical backbone of alternating silicon and oxygen atoms with methyl or vinyl side groups. The methyl group in the side chains contribute to the hydrophobicity of the material. The LSR used in the project has dimethyl chains. LSR has been specially used by the medical device manufacturers to produce more stable, flexible and physically implantable quality products. Some of the application of silicone rubber is in the manufacturing of precision molded parts, diaphragms, septa, valves, plungers etc. Since platinum cured, the rubber has long shelf life with excellent chemical resistance.

## 4.2. Basic properties:

LSR used in the molding procedure was manufactured by Applied Silicone Corporation. The LSR came in two parts A and B, both being colorless, translucent and ultraviolet- and strain resistant. The material has the property to withstand high strength which is basic requirement for the pump development. To obtain the elastomer of desired toughness and rubbery texture both the parts A and B (figure 16) are to mixed in equal

proportion [12]. Despite of its virtual unlimited shelf life, the manufacturer suggest a shelf life upto 3 years for molded parts. The specific material used for the project from Applied Silicone Corporation has long term implantation capacity with high durability.


Figure 16: Packed Liquid silicone rubber as Part A and Part B.

One of the eye catching property of LSR is its biocompatibility. It is also hypoallergenic which implies that the implanted device or part will have minimum risk of developing an allergic reaction in the host body. It also has anti-bacterial and fungal properties resulting in minimal chances of developing any bacterial or fungal infections in the body. LSR belongs to a family of thermosets resulting in its property of withstanding wide range of temperature change ( -55$^{o}$C to 200$^{o}$C) allowing it to go through sterilization processes like autoclaving without changing its properties.

**4.3. LSR usage in laboratory:**

When mixed part A and part B in a 1:1 ratio under proper conditions and with required specific inner dimensions of the pump, two molds were made.

Figure 17 shows the molds made in the laboratory to study the device inner dynamics.

Figure 17: The two inner surface moulds made out of LSR

Further specific details of the properties of LSR from applied silicone corporation can be referred by the material safety data sheet (MSDS) of LSR systems from Appendix 1.

# CHAPTER 5

# DISCUSSION AND CONCLUSION

A potential working prototype of a heart mimicking pump have been proposed. To overcome the disadvantages of the current pumps available in the market, different actuation methods and blood fluid dynamics have been studied. A vast majority of heart assist devices are complete bypass or large volume pumps that can cause significant blood cell damage which results in the thrombosis and thereby causes blood clotting and increases stroke/ heart failure chances.

The proposed design of the pump works on the basis of mimicking the actual heart pumping mechanism: the pulsatile compression and decompression. This mechanism helps in achieving the required flow rate with a less turbulent blood flow resulting in minimal blood cell damage. The pump under development focuses a lot on the prevention of damage to the blood cells due to the turbulent flow of blood in other rotary and displacement pumps. The pumping action of the device is created by the pressure gradient against the continuous flow. In general, continuous flow pumps produces non-pulsatile flow using a rotor which generally contains magnets that leads to a turbulence in the blood.

The use of COMSOL simulation has aided to the better understanding of the design and the blood flow dynamics. The studies through COMSOL simulation has suggested that the proposed design provides a lesser shear rate as compared to other heart assist devices which added as an advantage. The design also includes sphincter-like valves that also helps minimize the thrombosis which in other pumps is a result of turbulence. The design takes special care into the biocompatibility of the material used and in order to

achieve this, it is can be coated with a layer of polyethylene oxide (PEO) which reduces the protein interaction on the pump interior surfaces.

The actual compression and decompression of the pump caused by the sphincter valves are controlled by pneumatic cuffs. To improve the design capacities both shape memory alloys and pneumatic cuffs implementation has been studied. The pneumatic cuffs around the pump can help in the inflation and the deflation of the sphincter valves. This results in a zonal compression of the pump which give an optimized blood flow rate. Further research has been carried out with the prototype having pneumatic cuffs rather than shape memory alloys as it provides simple sequencing on the two way valves. Accelerometers are incorporated to the design that analyses the pump body motion and can provide a feedback of the pumping action. Further a cluster of pumps can be packed together to obtain complex flow patterns.

This blood pump design can provide upto 20% of cardiac assist to persons suffering from congestive heart failure and other heart abnormalities where extra blood pumping assistance is required. The pump also has minimum pressure capacity of 120mmHg at 50-150 heart beats per minute. Also the design suggested and in development have a broad spectrum of uses. This design is not just limited to the arterial to arterial pumping but can be used for physiological fluidic maintenance, intravenous drug delivery and pressure maintenance and to other applications where a low turbulence and shear stress is required.

## APPENDIX 1

MATERIAL SAFETY DATA SHEET

LIQUID SILICONE RUBBER (LSR) SYSTEMS

### I. PRODUCT IDENTIFICATION

A. Manufactured by:

APPLIED SILICONE CORPORATION
270 QUAIL COURT
SANTA PAULA, CA 93060
Telephone: (805) 525-5657
Fax: (805) 933-1675

For Chemical Emergency
Please call CHEMTREC
(800) 424-9300

B. Trade Name: Liquid Silicone Rubber (LSR), Part A and Part B

C. Chemical Name and Synonyms: Part A: reinforced dimethyl methylvinyl siloxanes. Part B: reinforced dimethyl methylhydrogen siloxanes.

D. Chemical Formula: N/A (polymeric), both Part A and Part B.

E. Chemical Family: Part A: reinforced organopolysiloxane, Part B: organopolysiloxane

F. DOT (CFR 49) Hazard Classification: Not hazardous per CFR 49

### II. PRODUCT COMPOSITION

Dimethyl Silicone Elastomer Base, 100%

### III. PHYSICAL PROPERTIES – PART A

A. Boiling Point: >260 $^{o}$C

B. Specific Gravity (water = 1): 1.1

C. Vapor Pressure at 25 $^{o}$C: >1 mm Hg - essentially non-volatile

D. Vapor Density (Air = 1): N/A - essentially non-volatile

E. Water Solubility: nil

F. Evaporation Rate (Ethyl Ether = 1): nil

G. Appearance and Odor: Colorless, translucent, viscous, paste

## III. PHYSICAL PROPERTIES - PART B

A. Boiling Point: >260°C

B. Specific Gravity (water = 1): 1.1

C. Vapor Pressure at 25°C: negligible - essentially non-volatile

D. Vapor Density (Air = 1): N/A - essentially non-volatile

E. Water Solubility: nil

F. Evaporation Rate (Ethyl Ether = 1): N/A

G. Appearance and Odor: Colorless, translucent, viscous, paste.

## IV. FIRE AND EXPLOSION INFORMATION – PART A AND PART B

A. Flash Point (Open Cup): Part A: 190°C; Part B: 95°C

B. Flammable Limits in Air, % Volume: Not measured

C. Extinguishing Media: Use water fog, dry chemical, foam, or $CO_2$

D. Special Fire Fighting Procedures: Fire fighters should wear self-contained breathing apparatus and full protective clothing. Use water spray to cool nearby containers.

E. Unusual Fire and Explosion Hazards: Part B may generate Hydrogen gas to create an explosion hazard.

## V. HEALTH HAZARD AND PROTECTION DATA - PART A AND PART B

A. Personal Protection Recommended: Wear protective goggles to prevent eye contact. Under recommended conditions of use, no other protection should be required.

B. Signs and Symptoms of Exposure: The primary route of exposure is eye contact. Direct eye contact can cause a transitory irritation, but it is not injurious. This irritation may persist for up to 24 hours.

Experience with this material has not indicated any serious effects related to exposure by any route.

C. First Aid for Exposure:

1. Eye contact: Flush with water. Get medical attention if irritation persists.

2. Skin contact: Not considered a potential hazard. If irritation occurs, wash thoroughly with soap and water.

3. Ingestion: Get medical attention

4. Inhalation: Not considered a potential hazard.

D. Occupational Exposure Limits: Because of the low health hazard, no exposure limits have been established.
E. Eye irritant in raw state.
F. Medical Conditions Generally Aggravated by Exposure: Pre-existing eye disorders.
G. Toxicity: Because of the low toxicity, specific toxicity data is unavailable.

## VI. SPILL AND LEAK PROCEDURES - PART A AND PART B

Use personal protection recommended in section V to prevent personnel exposure.

Even small amounts of spilled material may present a slip hazard.

As required, dike with soil or other absorbent materials to prevent spread of spill. Mop or wipe up and place in appropriate containers and/or place absorbent material on spill and transfer absorbed solvent to appropriate containers. Clean any remaining slippery surfaces. Mop or swab with appropriate solvent or wash with mild caustic detergents.

## VII. REACTIVITY DATA - PART A AND PART B

A. Stability: This material is chemically stable. Hazardous polymerization will not occur.

B. Materials to Avoid: Strong alkali contact with Part B may generate flammable hydrogen gas.

C. Hazardous Decomposition Products: Burning may liberate carbon monoxide, carbon dioxide and silicone dioxide.

## VIII. OTHER INFORMATION AND PRECAUTIONS - PART A AND PART B

Store in a cool, dry place. Keep container closed and keep away from heat and flame. Do not lay container on its side.

To the best of our knowledge this material does not contain any substances listed by the state of California to cause cancer, birth defects, or other reproductive effects.

When this material is discarded, as received, it is not classified as a RCRA hazardous waste. state and local laws may impose additional regulatory requirements regarding disposal.

Consult and comply with federal, state, and local regulations concerning any release of hazardous materials into the water, water piping systems, ground, or air. Consult and comply with federal, state, and local regulations concerning removal of waste.

All information appearing herein is based upon data considered to be accurate. However, no warranty is expressed or implied regarding the accuracy of these data or the results to be obtained from the use thereof.

**APPENDIX 2**
COMSOL SIMULATION RESULT

## 1. Model Properties

| Property | Value |
|---|---|
| Model name | Peristaltic Pump |
| Author | COMSOL |
| Company | COMSOL |
| Department | |
| Reference | Copyright (c) 1998-2008 by COMSOL AB |
| URL | www.comsol.com |
| Saved date | Apr 10, 2015 2:16:34 PM |
| Creation date | Nov 17, 2008 7:12:05 PM |
| COMSOL version | COMSOL 3.5.0.603 |

Application modes and modules used in this model:

- Geom1 (Axial symmetry (2D))
  - Axial Symmetry, Stress-Strain
  - Moving Mesh (ALE)
  - Non-Newtonian Flow (Chemical Engineering Module)

### 1.1. Model description

Peristaltic Pump

Rollers are squeezing a flexible tube in this model of a peristaltic pump. The compression drives a fluid through the tube. The motion of the fluid is computed with the help of a Moving Mesh application mode.

## 2. Constants

| Name | Expression | Value | Description |
|---|---|---|---|
| t_on | 0.3[s] | | Time when roll is engaged |
| t_off | 1.2[s] | | Time when roll is disengaged |
| dt | 0.2[s] | | Time to reach full force |
| z0 | 0.03[m] | | z coordinate where roll starts |
| v0 | 0.03[m/s] | | Vertical velocity of roll |
| width | 0.01[m] | | Width of Gaussian force distribution |
| Ttot | 1.5[s] | | Total time for a pump cycle |
| Lmax | 4e6[N/m^2] | | Max load |

## 3. Geometry

Number of geometries: 1

### 3.1. Geom1

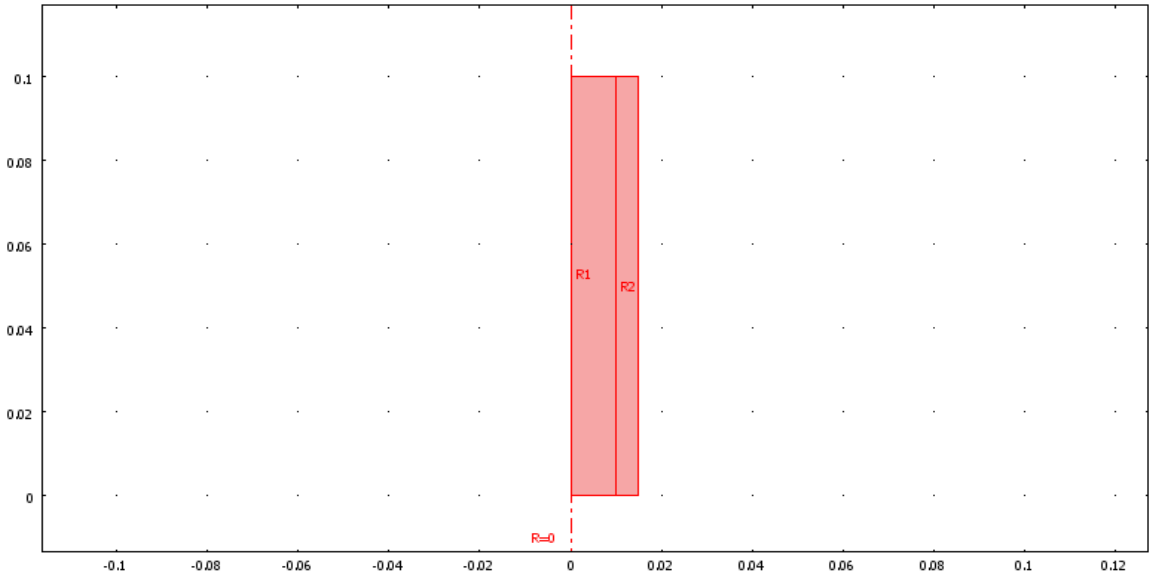


#### 3.1.1. Point mode

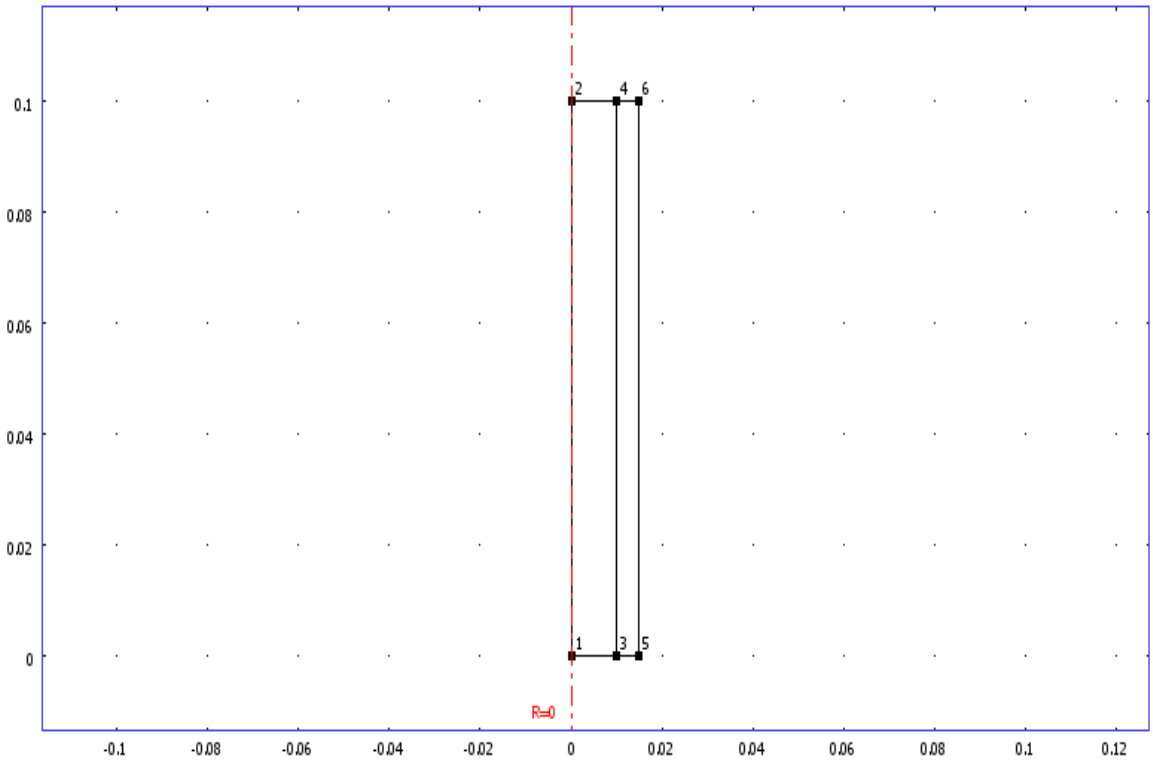

### 3.1.2. Boundary mode

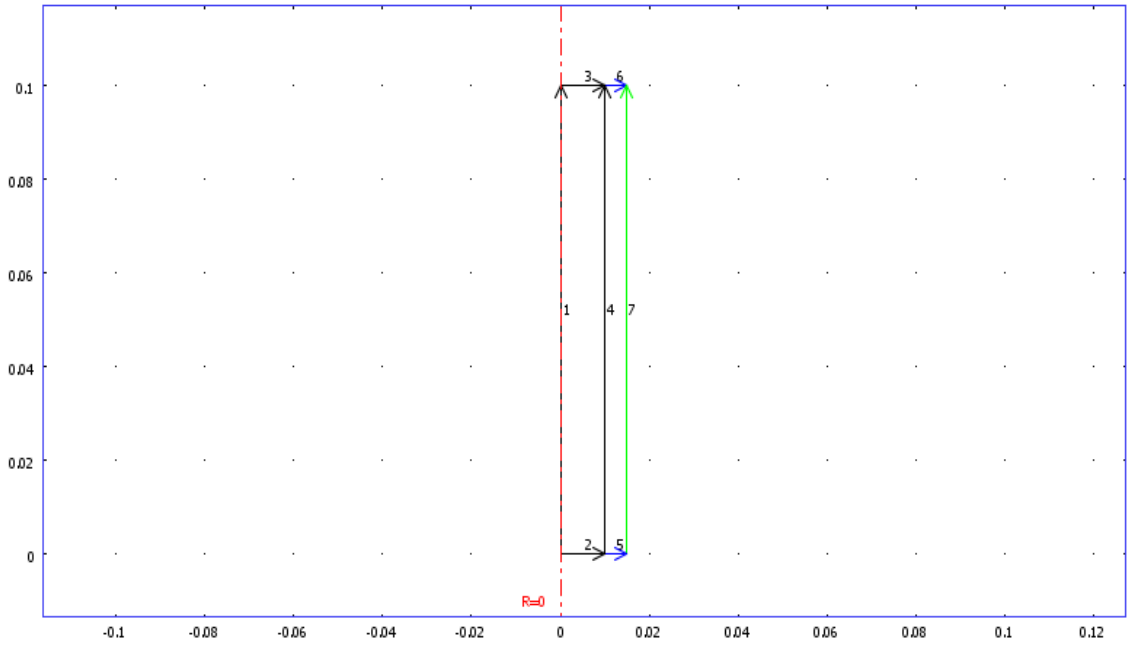


### 3.1.3. Subdomain mode

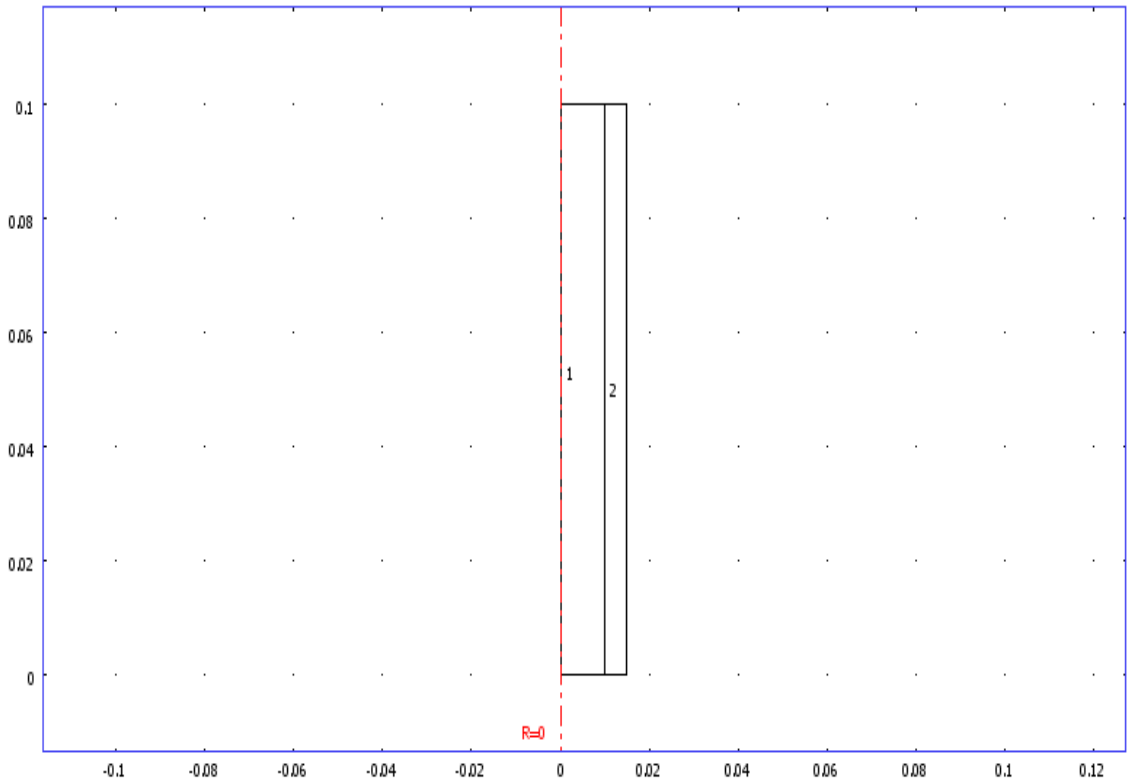

**4. Geom1**
Space dimensions: Axial symmetry (2D)
Independent variables: R, PHI, Z

**4.1. Mesh**
**4.1.1. Mesh Statistics**

| | |
|---|---|
| Number of degrees of freedom | 7741 |
| Number of mesh points | 517 |
| Number of elements | 916 |
| Triangular | 916 |
| Quadrilateral | 0 |
| Number of boundary elements | 166 |
| Number of vertex elements | 6 |
| Minimum element quality | 0.924 |
| Element area ratio | 0.398 |

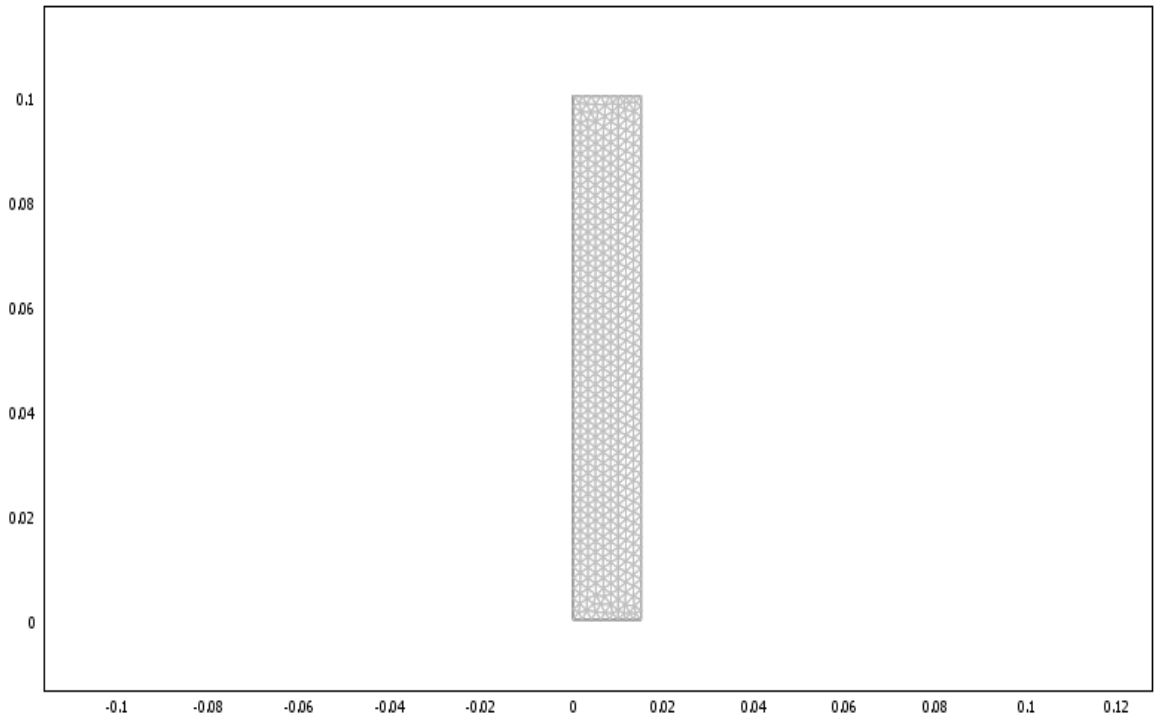


**4.2. Application Mode: Axial Symmetry, Stress-Strain (axi)**
Application mode type: Axial Symmetry, Stress-Strain
Application mode name: axi

### 4.2.1. Application Mode Properties

| Property | Value |
|---|---|
| Default element type | Lagrange - Quadratic |
| Analysis type | Transient |
| Specify eigenvalues using | Eigenfrequency |
| Frame | Frame (ref) |
| Weak constraints | Off |
| Constraint type | Ideal |

### 4.2.2. Variables

Dependent variables: uor, w
Shape functions: shlag(2,'uor'), shlag(2,'w')
Interior boundaries not active

### 4.2.3. Boundary Settings

| Boundary | | 4 | 5-6 | 7 |
|---|---|---|---|---|
| Edge load (force/area) R-dir. (Fr) | $N/m^2$ | 0 | 0 | **-0.5*Lmax*flc2hs((t-t_on)[1/s],dt[1/s])*gauss((z-0.05)[1/m],width[1/m])*flc2hs((t_off-t)[1/s],dt[1/s])** |
| Hr | 1 | 0 | **1** | 0 |
| Hz | 1 | 0 | **1** | 0 |

### 4.2.4. Subdomain Settings

| Subdomain | | 2 |
|---|---|---|
| Young's modulus (E) | Pa | **2e9[Pa] (Nylon)** |
| Density (rho) | $kg/m^3$ | **1150[kg/m^3] (Nylon)** |

## 4.3. Application Mode: Moving Mesh (ALE) (ale)

Application mode type: Moving Mesh (ALE)
Application mode name: ale

### 4.3.1. Application Mode Properties

| Property | Value |
|---|---|
| Default element type | Lagrange - Quadratic |
| Smoothing method | Winslow |

| | |
|---|---|
| Analysis type | Transient |
| Allow remeshing | Off |
| Defines frame | Frame (ale) |
| Original reference frame | Frame (ale) |
| Motion relative to | Frame (ref) |
| Weak constraints | On |
| Constraint type | Non-ideal |

### 4.3.2. Variables

Dependent variables:
Shape functions: shlag(2,'lm3'), shlag(2,'lm4'), shlag(2,'r'), shlag(2,'z')
Interior boundaries not active

### 4.3.3. Boundary Settings

| Boundary | | 1 | 2-3 | 4 |
|---|---|---|---|---|
| Type | | Mesh displacement | Mesh displacement | Mesh displacement |
| Mesh displacement (deform) | m | {0;0} | {0;0} | **{uaxi_axi;w}** |
| defflag | | **{1;0}** | **{0;1}** | **{1;1}** |

### 4.3.4. Subdomain Settings

| Subdomain | | 1 | 2 |
|---|---|---|---|
| Shape functions (shape) | | **shlag(2,'lm3') shlag(2,'lm4') shlag(2,'r') shlag(2,'z')** | **shlag(2,'lm3') shlag(2,'lm4') shlag(2,'r') shlag(2,'z')** |
| Integration order (gporder) | | **4 4** | **4 4** |
| type | | Free displacement | **Prescribed displacement** |
| Displacement expressions (presexpr) | m | {0;0} | **{uaxi_axi;w}** |

| Subdomain initial value | | 1 | 2 |
|---|---|---|---|
| Spatial coordinate (r) | m | rinit_ale | rinit_ale |
| Spatial coordinate (z) | m | zinit_ale | zinit_ale |

### 4.4. Application Mode: Non-Newtonian Flow (chns)

Application mode type: Non-Newtonian Flow (Chemical Engineering Module)
Application mode name: chns

#### 4.4.1. Scalar Variables

| Name | Variable | Value | Unit | Description |
|---|---|---|---|---|
| visc_vel_fact | visc_vel_fact_chns | 10 | 1 | Viscous velocity factor |

#### 4.4.2. Application Mode Properties

| **Property** | **Value** |
|---|---|
| Default element type | Lagrange - $P_2$ $P_1$ |
| Analysis type | Transient |
| Corner smoothing | Off |
| Weakly compressible flow | Off |
| Turbulence model | None |
| Realizability | Off |
| Non-Newtonian flow | On |
| Brinkman on by default | Off |
| Two-phase flow | Single-phase flow |
| Swirl velocity | Off |
| Frame | Frame (ale) |
| Weak constraints | On |
| Constraint type | Ideal |

#### 4.4.3. Variables

Dependent variables: u, v, w2, p, logk2, logd2, logw2, phi2, psi2, nrw2, nzw2
Shape functions: shlag(2,'lm5'), shlag(2,'lm6'), shlag(1,'lm8'), shlag(2,'u'), shlag(2,'v'), shlag(1,'p')
Interior boundaries not active

#### 4.4.4. Boundary Settings

| Boundary | | 1 | 2-3 | 4 |
|---|---|---|---|---|
| Type | | Symmetry boundary | Open boundary | Inlet |
| velType | | U0in | U0in | **u0** |

| | | | | |
|---|---|---|---|---|
| r-velocity (u0) | m/s | 0 | 0 | **uaxi_t_axi** |
| z-velocity (v0) | m/s | 0 | 0 | **wt** |

### 4.4.5. Subdomain Settings

| | | |
|---|---|---|
| Subdomain | | 1 |
| Shape functions (shape) | | **shlag(2,'lm5') shlag(2,'lm6') shlag(1,'lm8') shlag(2,'u') shlag(2,'v') shlag(1,'p')** |
| Integration order (gporder) | | **4 4 2** |
| Constraint order (cporder) | | **2 2 1** |
| Model parameter (m) | | **0.0161** |
| Model parameter (n) | 1 | **.63** |
| idon | | **1** |
| cdon | | **0** |

## 5. Materials/Coefficients Library

### 5.1. Nylon

| **Parameter** | **Value** |
|---|---|
| Heat capacity at constant pressure (C) | 1700[J/(kg*K)] |
| Young's modulus (E) | 2e9[Pa] |
| Thermal expansion coeff. (alpha) | 280e-6[1/K] |
| Relative permittivity (epsilonr) | 4 |
| Thermal conductivity (k) | 0.26[W/(m*K)] |
| Density (rho) | 1150[kg/m^3] |

## 6. Global Equations

| **Name (u)** | **Equation** | **Init (u)** | **Init (ut)** | **Description** |
|---|---|---|---|---|
| netflow | netflowt-(inflow+outflow)/(2*Ttot) | 0 | 0 | |

## 7. Integration Coupling Variables

### 7.1. Geom1

#### 7.1.1. Source Boundary: 2

| Name | Value |
|---|---|
| Variable name | inflow |
| Expression | 2*pi*r*v |
| Order | 4 |
| Global | Yes |

#### 7.1.2. Source Boundary: 3

| Name | Value |
|---|---|
| Variable name | outflow |
| Expression | 2*pi*r*v |
| Order | 4 |
| Global | Yes |

#### 7.1.3. Source Subdomain: 1

| Name | Value |
|---|---|
| Variable name | Vol |
| Expression | 2*pi*r |
| Order | 4 |
| Global | Yes |

## 8. Functions

| Function | Expression | Derivatives | Complex output |
|---|---|---|---|
| gauss(x,sigma) | 1/(sigma*sqrt(2*pi))*exp(-x^2/(2*sigma^2)) | d(1/(sigma*sqrt(2*pi))*exp(-x^2/(2*sigma^2)),x), d(1/(sigma*sqrt(2*pi))*exp(-x^2/(2*sigma^2)),sigma) | false |

**9. Solver Settings**
Solve using a script: off

| | |
|---|---|
| Analysis type | Transient |
| Auto select solver | On |
| Solver | Time dependent |
| Solution form | Automatic |
| Symmetric | Auto |
| Adaptive mesh refinement | Off |
| Optimization/Sensitivity | Off |
| Plot while solving | Off |

**9.1. Direct (PARDISO)**
Solver type: Linear system solver

| **Parameter** | **Value** |
|---|---|
| Preordering algorithm | Nested dissection |
| Row preordering | On |
| Bunch-Kaufmann | Off |
| Pivoting perturbation | 1.0E-8 |
| Relative tolerance | 1.0E-6 |
| Factor in error estimate | 400.0 |
| Check tolerances | Off |

**9.2. Time Stepping**

| **Parameter** | **Value** |
|---|---|
| Times | range(0,0.01,1.5) |
| Relative tolerance | 0.01 |
| Absolute tolerance | 1e-3 |
| Times to store in output | Specified times |
| Time steps taken by solver | Strict |
| Maximum BDF order | 2 |
| Singular mass matrix | Maybe |
| Consistent initialization of DAE systems | Backward Euler |
| Error estimation strategy | Exclude algebraic |
| Allow complex numbers | Off |

### 9.3. Advanced

| Parameter | Value |
|---|---|
| Constraint handling method | Elimination |
| Null-space function | Automatic |
| Automatic assembly block size | On |
| Assembly block size | 1000 |
| Use Hermitian transpose of constraint matrix and in symmetry detection | Off |
| Use complex functions with real input | Off |
| Stop if error due to undefined operation | On |
| Store solution on file | Off |
| Type of scaling | Automatic |
| Manual scaling | |
| Row equilibration | On |
| Manual control of reassembly | Off |
| Load constant | On |
| Constraint constant | On |
| Mass constant | On |
| Damping (mass) constant | On |
| Jacobian constant | On |
| Constraint Jacobian constant | On |

## 10. Postprocessing

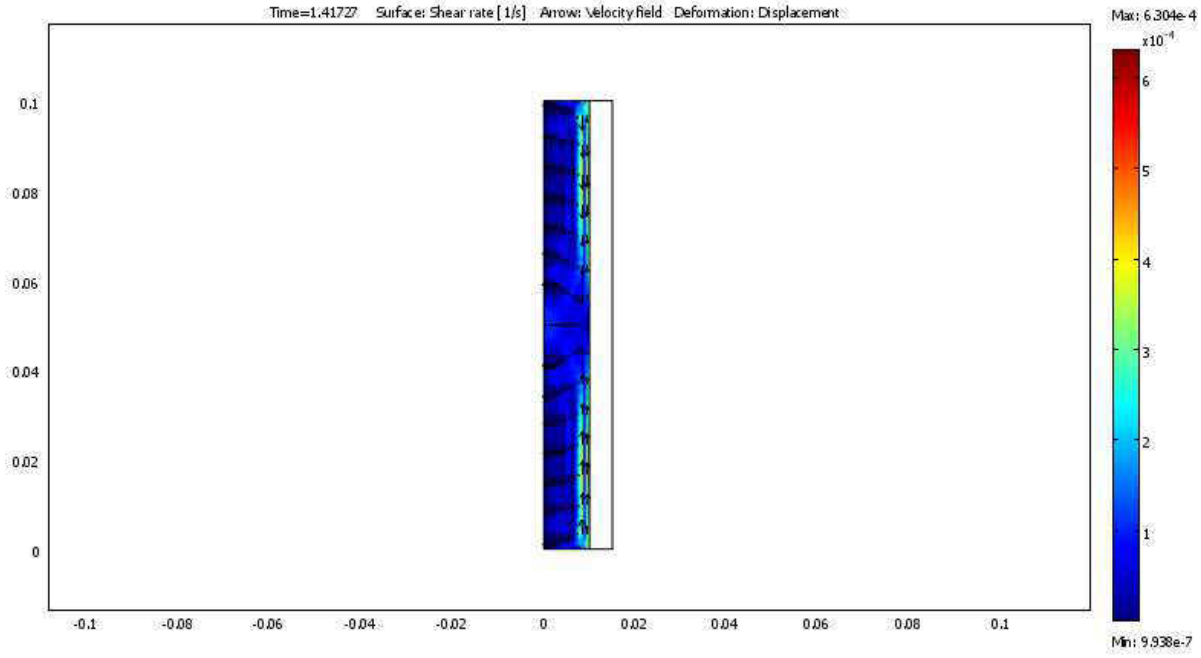

## 11. Variables

### 11.1. Point

#### 11.1.1. Point 1-2

| Name | Description | Unit | Expression |
|---|---|---|---|
| RFR_axi | Reaction force R-dir. | N | |
| RFZ_axi | Reaction force Z-dir. | N | |
| FRg_axi | Point load in global R dir. | N | |
| FZg_axi | Point load in global Z dir. | N | |
| disp_axi | Total displacement | M | |
| uaxi_axi | R-displacement | m | |
| uaxiR_axi | R derivative of R-displacement | 1 | |
| uaxiZ_axi | Z derivative of R displacement | 1 | |
| uaxi_t_axi | R-velocity | m/s | |
| uaxi_tt_axi | R-acceleration | m/s^2 | |
| rinit_ale | r coordinate initial value | m | R |
| zinit_ale | z coordinate initial value | m | Z |

#### 11.1.2. Point 3-6

| Name | Description | Unit | Expression |
|---|---|---|---|
| RFR_axi | Reaction force R-dir. | N | if(R>0,2 * reacf(uor) * pi/R,0) |
| RFZ_axi | Reaction force Z-dir. | N | 2 * reacf(w) * pi |
| FRg_axi | Point load in global R dir. | N | 0 |
| FZg_axi | Point load in global Z dir. | N | 0 |
| disp_axi | Total displacement | m | sqrt(real(uaxi_axi)^2+real(w)^2) |
| uaxi_axi | R-displacement | m | uor * R |
| uaxiR_axi | R derivative of R-displacement | 1 | uorR * R+uor |
| uaxiZ_axi | Z derivative of R displacement | 1 | uorZ * R |
| uaxi_t_axi | R-velocity | m/s | uort * R |
| uaxi_tt_axi | R-acceleration | m/s^2 | uortt * R |
| rinit_ale | r coordinate initial value | m | R |
| zinit_ale | z coordinate initial value | m | Z |

## 11.2. Boundary

### 11.2.1. Boundary 1-3

| Name | Description | Unit | Expression |
|---|---|---|---|
| RFR_axi | Reaction force R-dir. | N | |
| RFZ_axi | Reaction force Z-dir. | N | |
| FRg_axi | Edge load in global R-dir. | N/m^2 | |
| FZg_axi | Edge load in global Z-dir. | N/m^2 | |
| disp_axi | Total displacement | m | |
| uaxi_axi | R-displacement | m | |
| uaxiR_axi | R derivative of R-displacement | 1 | |
| uaxiZ_axi | Z derivative of R displacement | 1 | |
| uaxi_t_axi | R-velocity | m/s | |
| uaxi_tt_axi | R-acceleration | m/s^2 | |
| TaR_axi | Surface traction (force/area) in R dir. | Pa | |
| TaZ_axi | Surface traction (force/area) in Z dir. | Pa | |
| rinit_ale | r coordinate initial value | m | R |
| zinit_ale | z coordinate initial value | m | Z |
| K_r_chns | Viscous force per area, r component | Pa | eta_chns * (2 * nr_chns * ur+nz_chns * (uz+vr)) |
| T_r_chns | Total force per area, r component | Pa | -nr_chns * p+2 * nr_chns * eta_chns * ur+nz_chns * eta_chns * (uz+vr) |
| K_z_chns | Viscous force per area, z component | Pa | eta_chns * (nr_chns * (vr+uz)+2 * nz_chns * vz) |
| T_z_chns | Total force per area, z component | Pa | -nz_chns * p+nr_chns * eta_chns * (vr+uz)+2 * nz_chns * eta_chns * vz |

### 11.2.2. Boundary 4

| Name | Description | Unit | Expression |
|---|---|---|---|
| RFR_axi | Reaction force R-dir. | N | if(R>0,2 * reacf(uor) * pi/R,0) |
| RFZ_axi | Reaction force Z-dir. | N | 2 * reacf(w) * pi |
| FRg_axi | Edge load in global | N/m^2 | 0 |

| | | | |
|---|---|---|---|
| | R-dir. | | |
| FZg_axi | Edge load in global Z-dir. | N/m^2 | 0 |
| disp_axi | Total displacement | M | sqrt(real(uaxi_axi)^2+real(w)^2) |
| uaxi_axi | R-displacement | M | uor * R |
| uaxiR_axi | R derivative of R-displacement | 1 | uorR * R+uor |
| uaxiZ_axi | Z derivative of R displacement | 1 | uorZ * R |
| uaxi_t_axi | R-velocity | m/s | uort * R |
| uaxi_tt_axi | R-acceleration | m/s^2 | uortt * R |
| TaR_axi | Surface traction (force/area) in R dir. | Pa | sR_axi * nR_axi+sRZ_axi * nZ_axi |
| TaZ_axi | Surface traction (force/area) in Z dir. | Pa | sRZ_axi * nR_axi+sZ_axi * nZ_axi |
| rinit_ale | r coordinate initial value | M | R |
| zinit_ale | z coordinate initial value | M | Z |
| K_r_chns | Viscous force per area, r component | Pa | eta_chns * (2 * nr_chns * ur+nz_chns * (uz+vr)) |
| T_r_chns | Total force per area, r component | Pa | -nr_chns * p+2 * nr_chns * eta_chns * ur+nz_chns * eta_chns * (uz+vr) |
| K_z_chns | Viscous force per area, z component | Pa | eta_chns * (nr_chns * (vr+uz)+2 * nz_chns * vz) |
| T_z_chns | Total force per area, z component | Pa | -nz_chns * p+nr_chns * eta_chns * (vr+uz)+2 * nz_chns * eta_chns * vz |

### 11.2.3. Boundary 5-6

| Name | Description | Unit | Expression |
|---|---|---|---|
| RFR_axi | Reaction force R-dir. | N | if(R>0,2 * reacf(uor) * pi/R,0) |
| RFZ_axi | Reaction force Z-dir. | N | 2 * reacf(w) * pi |
| FRg_axi | Edge load in global R-dir. | N/m^2 | 0 |
| FZg_axi | Edge load in global Z-dir. | N/m^2 | 0 |
| disp_axi | Total displacement | m | sqrt(real(uaxi_axi)^2+real(w)^2) |
| uaxi_axi | R-displacement | m | uor * R |
| uaxiR_axi | R derivative of R-displacement | 1 | uorR * R+uor |
| uaxiZ_axi | Z derivative of R displacement | 1 | uorZ * R |

| | | | |
|---|---|---|---|
| uaxi_t_axi | R-velocity | m/s | uort * R |
| uaxi_tt_axi | R-acceleration | m/s^2 | uortt * R |
| TaR_axi | Surface traction (force/area) in R dir. | Pa | sR_axi * nR_axi+sRZ_axi * nZ_axi |
| TaZ_axi | Surface traction (force/area) in Z dir. | Pa | sRZ_axi * nR_axi+sZ_axi * nZ_axi |
| rinit_ale | r coordinate initial value | m | R |
| zinit_ale | z coordinate initial value | m | Z |
| K_r_chns | Viscous force per area, r component | Pa | |
| T_r_chns | Total force per area, r component | Pa | |
| K_z_chns | Viscous force per area, z component | Pa | |
| T_z_chns | Total force per area, z component | Pa | |

### 11.2.4. Boundary 7

| **Name** | **Description** | **Unit** | **Expression** |
|---|---|---|---|
| RFR_axi | Reaction force R-dir. | N | if(R>0,2 * reacf(uor) * pi/R,0) |
| RFZ_axi | Reaction force Z-dir. | N | 2 * reacf(w) * pi |
| FRg_axi | Edge load in global R-dir. | N/m^2 | FR_axi |
| FZg_axi | Edge load in global Z-dir. | N/m^2 | 0 |
| disp_axi | Total displacement | m | sqrt(real(uaxi_axi)^2+real(w)^2) |
| uaxi_axi | R-displacement | m | uor * R |
| uaxiR_axi | R derivative of R-displacement | 1 | uorR * R+uor |
| uaxiZ_axi | Z derivative of R displacement | 1 | uorZ * R |
| uaxi_t_axi | R-velocity | m/s | uort * R |
| uaxi_tt_axi | R-acceleration | m/s^2 | uortt * R |
| TaR_axi | Surface traction (force/area) in R dir. | Pa | sR_axi * nR_axi+sRZ_axi * nZ_axi |
| TaZ_axi | Surface traction (force/area) in Z dir. | Pa | sRZ_axi * nR_axi+sZ_axi * nZ_axi |
| rinit_ale | r coordinate initial value | m | R |
| zinit_ale | z coordinate initial value | m | Z |
| K_r_chns | Viscous force per area, r component | Pa | |
| T_r_chns | Total force per area, r | Pa | |

| | | | |
|---|---|---|---|
| | component | | |
| K_z_chns | Viscous force per area, z component | Pa | |
| T_z_chns | Total force per area, z component | Pa | |

### 11.3. Subdomain

#### 11.3.1. Subdomain 1

| Name | Description | Unit | Expression |
|---|---|---|---|
| RFR_axi | Reaction force R-dir. | N | |
| RFZ_axi | Reaction force Z-dir. | N | |
| FRg_axi | Body load in global R-dir. | N/m^3 | |
| FZg_axi | Body load in global Z-dir. | N/m^3 | |
| disp_axi | Total displacement | M | |
| uaxi_axi | R-displacement | M | |
| uaxiR_axi | R derivative of R-displacement | 1 | |
| uaxiZ_axi | Z derivative of R displacement | 1 | |
| uaxi_t_axi | R-velocity | m/s | |
| uaxi_tt_axi | R-acceleration | m/s^2 | |
| sR_axi | sR normal stress global sys. | Pa | |
| sZ_axi | sZ normal stress global sys. | Pa | |
| sPHI_axi | sPHI normal stress | Pa | |
| sRZ_axi | sRZ shear stress global sys. | Pa | |
| eR_axi | eR normal strain global sys. | 1 | |
| eZ_axi | eZ normal strain global sys. | 1 | |
| ePHI_axi | ePHI normal strain | 1 | |
| eRZ_axi | eRZ shear strain | 1 | |

| | | | |
|---|---|---|---|
| | global sys. | | |
| sr_t_axi | Time der. of normal stress global sys. (sR) | Pa/s | |
| sz_t_axi | Time der. of normal stress global sys. (sZ) | Pa/s | |
| sphi_t_axi | Time der. of normal stress (sPHI) | Pa/s | |
| srz_t_axi | Time der. of shear stress global sys. (sRZ) | Pa/s | |
| er_t_axi | eR_t normal velocity strain global sys. | 1/s | |
| ez_t_axi | eZ_t normal velocity strain global sys. | 1/s | |
| ephi_t_axi | ePHI_t normal velocity strain | 1/s | |
| erz_t_axi | eRPHI_t shear velocity strain global sys. | 1/s | |
| mises_axi | von Mises stress | Pa | |
| Ws_axi | Strain energy density | J/m^3 | |
| evol_axi | Volumetric strain | 1 | |
| tresca_axi | Tresca stress | Pa | |
| rinit_ale | r coordinate initial value | m | R |
| zinit_ale | z coordinate initial value | m | Z |
| dr_ale | r-displacement | m | r-R |
| dz_ale | z-displacement | m | z-Z |
| U_chns | Velocity field | m/s | sqrt(u^2+v^2) |
| V_chns | Vorticity | 1/s | uz-vr |
| divU_chns | Divergence of velocity field | 1/s | ur+vz+u/r |
| sr_chns | Shear rate | 1/s | sqrt(0.5 * (4 * ur^2+2 * (uz+vr)^2+4 * vz^2+4 * u^2/(r+eps)^2)+eps) |

| | | | |
|---|---|---|---|
| cellRe_chns | Cell Reynolds number | 1 | rho_chns * U_chns * h_ale/eta_chns |
| res_u_chns | Equation residual for u | Pa | r * (rho_chns * (ut+u * ur+v * uz)+pr-F_r_chns)+2 * eta_chns * (u/r-ur)-eta_chns * r * (2 * urr+uzz+vrz) |
| res_v_chns | Equation residual for v | Pa | r * (rho_chns * (vt+u * vr+v * vz)+pz-F_z_chns)-eta_chns * (r * (vrr+uzr)+2 * r * vzz+uz+vr) |
| beta_r_chns | Convective field, r component | Pa*s | r * rho_chns * u |
| beta_z_chns | Convective field, z component | Pa*s | r * rho_chns * v |
| Dm_chns | Mean diffusion coefficient | kg/s | r * eta_chns |
| da_chns | Total time scale factor | kg/m^2 | r * rho_chns |
| taum_chns | GLS time-scale | m^3*s/kg | nojac(1/max(2 * rho_chns * sqrt(emetric_ale(u-rt,v-zt)),48 * eta_chns/h_ale^2)) |
| tauc_chns | GLS time-scale | m^2/s | 0.5 * nojac(if((u-rt)^2+(v-zt)^2<="" td=""> |
| res_p_chns | Equation residual for p | kg/(m^2*s) | rho_chns * r * divU_chns |

### 11.3.2. Subdomain 2

| **Name** | **Description** | **Unit** | **Expression** |
|---|---|---|---|
| RFR_axi | Reaction force R-dir. | N | if(R>0,2 * reacf(uor) * pi/R,0) |
| RFZ_axi | Reaction force Z-dir. | N | 2 * reacf(w) * pi |
| FRg_axi | Body load in global R-dir. | N/m^3 | 0 |
| FZg_axi | Body load in global Z-dir. | N/m^3 | 0 |
| disp_axi | Total displacement | M | sqrt(real(uaxi_axi)^2+real(w)^2) |
| uaxi_axi | R-displacement | M | uor * R |
| uaxiR_axi | R derivative of R-displacement | 1 | uorR * R+uor |
| uaxiZ_axi | Z derivative of | 1 | uorZ * R |

| | | | |
|---|---|---|---|
| | R displacement | | |
| uaxi_t_axi | R-velocity | m/s | uort * R |
| uaxi_tt_axi | R-acceleration | m/s^2 | uortt * R |
| sR_axi | sR normal stress global sys. | Pa | E_axi * ((1-nu_axi) * eR_axi+nu_axi * ePHI_axi+nu_axi * eZ_axi)/((1+nu_axi) * (1-2 * nu_axi)) |
| sZ_axi | sZ normal stress global sys. | Pa | E_axi * (nu_axi * eR_axi+nu_axi * ePHI_axi+(1-nu_axi) * eZ_axi)/((1+nu_axi) * (1-2 * nu_axi)) |
| sPHI_axi | sPHI normal stress | Pa | E_axi * (nu_axi * eR_axi+(1-nu_axi) * ePHI_axi+nu_axi * eZ_axi)/((1+nu_axi) * (1-2 * nu_axi)) |
| sRZ_axi | sRZ shear stress global sys. | Pa | E_axi * eRZ_axi/(1+nu_axi) |
| eR_axi | eR normal strain global sys. | 1 | uorR * R+uor |
| eZ_axi | eZ normal strain global sys. | 1 | wZ |
| ePHI_axi | ePHI normal strain | 1 | uor |
| eRZ_axi | eRZ shear strain global sys. | 1 | 0.5 * (uorZ * R+wR) |
| sr_t_axi | Time der. of normal stress global sys. (sR) | Pa/s | E_axi * ((1-nu_axi) * er_t_axi+nu_axi * ephi_t_axi+nu_axi * ez_t_axi)/((1+nu_axi) * (1-2 * nu_axi)) |
| sz_t_axi | Time der. of normal stress global sys. (sZ) | Pa/s | E_axi * (nu_axi * er_t_axi+nu_axi * ephi_t_axi+(1-nu_axi) * ez_t_axi)/((1+nu_axi) * (1-2 * nu_axi)) |
| sphi_t_axi | Time der. of normal stress (sPHI) | Pa/s | E_axi * (nu_axi * er_t_axi+(1-nu_axi) * ephi_t_axi+nu_axi * ez_t_axi)/((1+nu_axi) * (1-2 * nu_axi)) |
| srz_t_axi | Time der. of shear stress global sys. (sRZ) | Pa/s | E_axi * erz_t_axi/(1+nu_axi) |
| er_t_axi | eR_t normal velocity strain global sys. | 1/s | uorRt * R+uort |
| ez_t_axi | eZ_t normal | 1/s | wZt |

| | | | |
|---|---|---|---|
| | velocity strain global sys. | | |
| ephi_t_axi | ePHI_t normal velocity strain | 1/s | uort |
| erz_t_axi | eRPHI_t shear velocity strain global sys. | 1/s | 0.5 * (uorZt * R+wRt) |
| mises_axi | von Mises stress | Pa | sqrt(sR_axi^2+sPHI_axi^2+sZ_axi^2-sR_axi * sPHI_axi-sPHI_axi * sZ_axi-sR_axi * sZ_axi+3 * sRZ_axi^2) |
| Ws_axi | Strain energy density | J/m^3 | 0.5 * (eR_axi * sR_axi+ePHI_axi * sPHI_axi+eZ_axi * sZ_axi+2 * eRZ_axi * sRZ_axi) |
| evol_axi | Volumetric strain | 1 | eR_axi+ePHI_axi+eZ_axi |
| tresca_axi | Tresca stress | Pa | max(max(abs(s1_axi-s2_axi),abs(s2_axi-s3_axi)),abs(s1_axi-s3_axi)) |
| rinit_ale | r coordinate initial value | M | R |
| zinit_ale | z coordinate initial value | M | Z |
| dr_ale | r-displacement | M | r-R |
| dz_ale | z-displacement | M | z-Z |
| U_chns | Velocity field | m/s | |
| V_chns | Vorticity | 1/s | |
| divU_chns | Divergence of velocity field | 1/s | |
| sr_chns | Shear rate | 1/s | |
| cellRe_chns | Cell Reynolds number | 1 | |
| res_u_chns | Equation residual for u | Pa | |
| res_v_chns | Equation residual for v | Pa | |
| beta_r_chns | Convective field, r component | Pa*s | |
| beta_z_chns | Convective field, z component | Pa*s | |
| Dm_chns | Mean diffusion | kg/s | |

| | | | |
|---|---|---|---|
| | coefficient | | |
| da_chns | Total time scale factor | kg/m^2 | |
| taum_chns | GLS time-scale | m^3*s/kg | |
| tauc_chns | GLS time-scale | m^2/s | |
| res_p_chns | Equation residual for p | kg/(m^2*s) | |

## REFERENCES

1. H.M Reul and M.Akdis , 'Blood pumps for circulatory support', Perfusion 2000; 15: 295–311.

2. Giersiepen M, Wurzinger LJ, Opitz R, Reul H, ' Estimation of shear-stress related blood damage in heart valve prostheses – in vitro comparison of 25 valves' 1990,13: 300–305.

3. Portner PM, ' A totally implantable ventricular assist device for end-stage heart disease', Berlin: Springer, 1984: 115–41.

4. Portner PM, 'A totally implantable heart assist system: the Novacor program. In: Akutsu T, Koyanagi H, eds. Heart replacement', Tokyo: Springer, 1993: 71–80.

5. Myers TJ, Dasee KA, Macris MP, Poirier VL, Cloy MJ, Frazier OH, ' Use of a left ventricular assist device in an outpatient setting', ASAIO J, 1994; 471–75.

6. Oguz K Baskurt, Herbert.J. Meiselman, 'Blood rheology and hemodynamics- Seminars in thrombosis and hemostasis',Vol29, 5, 2003.

7. Lowe GDO, Barbenel JC, ' Plasma and blood viscosity', In: Lowe GDO, ed. Clinical Blood Rheology,Vol 1, FL: CRC Press; 1988:11–44

8. Edward R Merrill, ' Rheology of blood. Physiological reviews', Vol 49. No.4, 1969.

9. Chien S, Sung LA, 'Physicochemical basis and clinical implications of red cell aggregation', Clinical Hemorheol 1987;7:71–91

10. Merrill, E. W., E. R. Gillilanp, G. R. Cokelet, H. Shin, A. Britten, and R. E. Wells, 'Rheology of human blood near and at zero flow-effects of temperature and hematocrit level',

Biophysics Journal, 3: 199-213, 1963.

11. Casson .N, ' Flow equations for pigment-oil suspensions of the printing ink type', In : Rheology of Disperse Systems, edited by C. C. Mills. New York: Pergamon,
1959, Chapt. 5.

12. Applied Silicone, "http://www.appliedsilicone.com/wp-content/uploads/2011/08/LSR-MS-002".

13. J. Ryan stanfield, Craig H. Selzman, *In vitro* pulsatility analysis of axial-flow and centrifugal-flow left ventricular assist devices, Journal of Biomechanical Engg., Vol 135, 2013.

# ABSTRACT

## NOVEL PULSATILE CARDIAC ASSIST PUMP

by

**LAKSHMI MOHANADAS**

**May 2015**

**Advisor:** Dr. Gregory W Auner

**Major:** Biomedical Engineering

**Degree:** Master of Science

The project involve the research and development of a pulsatile, complex or continuous flow in biological and non-biological systems implantable heart assist pump. Specifically as a 20% cardiac assist for persons from congestive heart failure and other cardiac abnormalities. The pulsatile cardiac assist pump would provide upto 20% of the blood pumping process from the venous supply to the arterial supply. Current pumps are largely complete bypass pumps or large volume pumps that produce significant long term blood cell damage resulting in thrombosis. Most are not pulsatile which offers a significant physiological advantage. The pump under development is designed to prevent thrombosis by utilizing a unique geometry and pumping actuation mechanism. As part of the research we first used COSMOL simulation to aid in the design and blood flow dynamics. From these results we have designed a working prototype that can be configured in a number of geometries or stages. This design utilizes biocompatible material, Polyethylene oxide (PEO), which minimized protein interaction with the interior pumping surface. Shape memory alloy

actuators compress the pumping chamber. Shape memory alloy actuators also actuate compression of the ingoing sphincter valve and outgoing sphincter valves. Pumping motion can be analyzed by accelerometers to provide optimized feedback and pump motion control. Zoned compression may allow optimal compression for blood flow. This type of pumping system biomimics actual heart compression and pulsation while the sphincter like valves minimizes thrombosis causing turbulent. A second actuation method may be employed utilizing pneumatic cuffs that inflate and compress the pump body and sphincter valves. The pump has a minimum of one hundred twenty mmHg pressure capabilities at fifty to one hundred and fifty beats per minute or in coordination with the compression and decompression rate of the heart as measured by blood pressure sensors or direct heart electro cardiac sensing. A cluster of pumps each independently controlled may be packaged for sequence or sequential actuation providing complex pumping and flow patterns or continuous pumping flow. Further the pumps may be independently actuated in a tandem configuration. As such the pump provides a broad field of use including but not limited to arterial to arterial pumping, drug delivery, physiological fluidic maintenance, intravenous delivery, pressure maintenance and drug manufacturing where low turbulence flow is required and any pulsatile, complex flow pattern or continuous flow pattern is required.

# AUTOBIOGRAPHICAL STATEMENT

**Lakshmi Mohanadas**

630 Merrick St, #201 Detroit, MI-48202 Email: fk2967@wayne.edu

---

## EDUCATIONAL QUALIFICATION:

* **Master of Science** in Biomedical Engineering - Wayne State University, May 2015.
Master Thesis Title: " Novel pulsatile cardiac assist pump".

* **Bachelor of Technology** in Biotechnology - University of Pune, India, May 2012.